Structural Analysis Part III - X-ray tools

Session 2:

X-ray scattering and diffraction

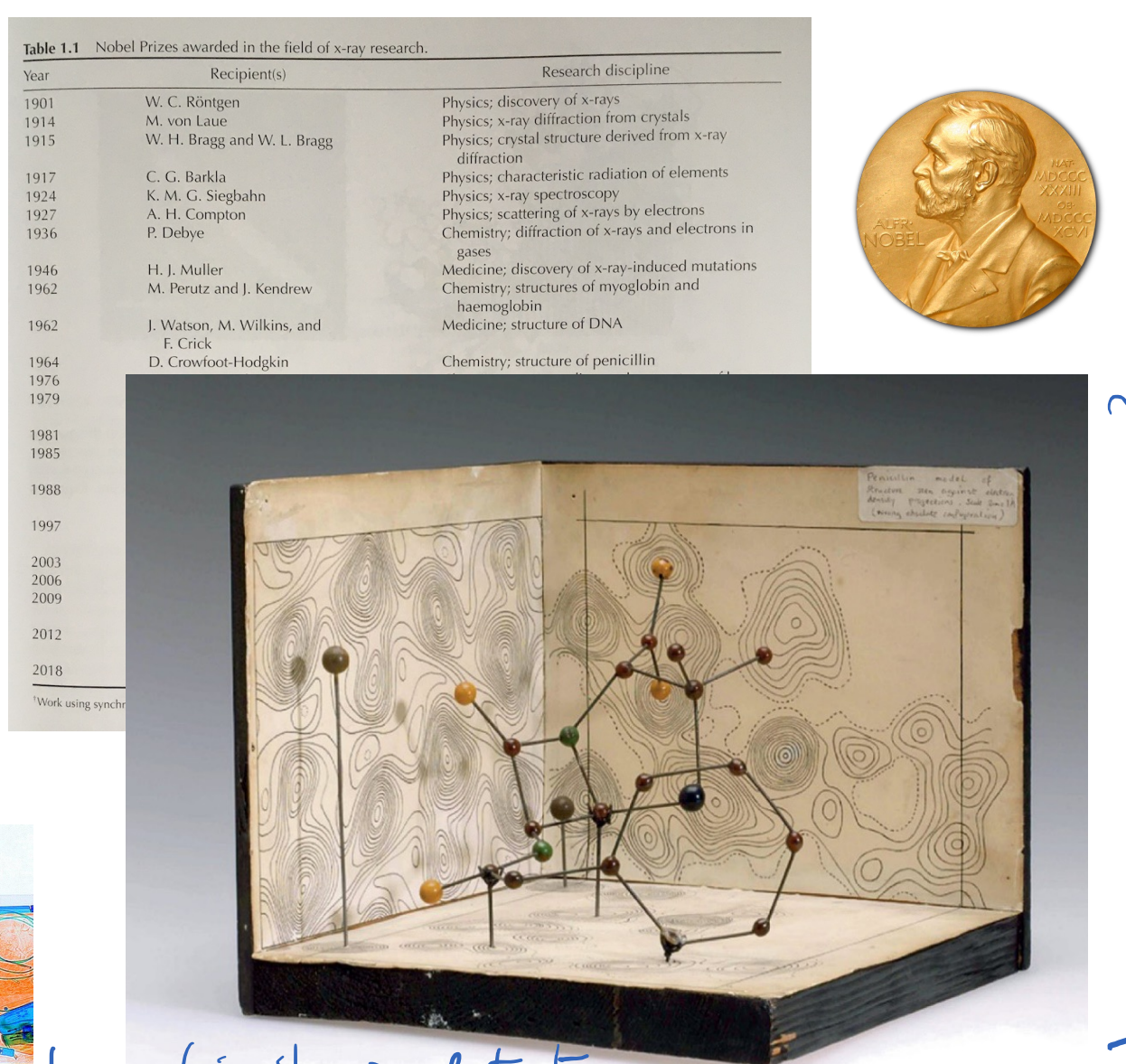
Discovery of X-rays triggered many technological and scientific developments

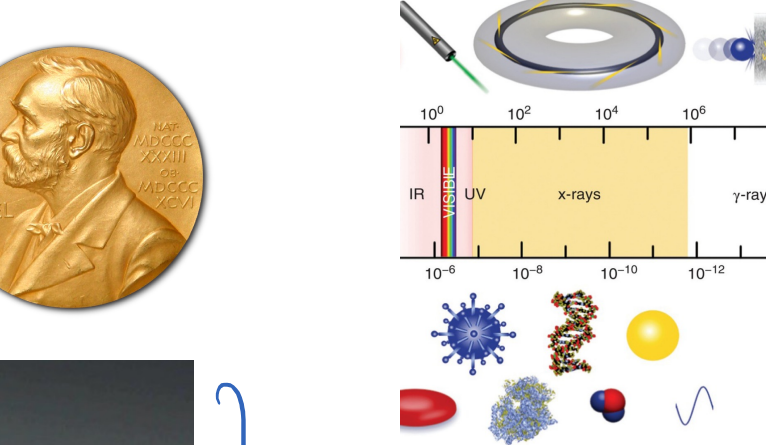












I matched to Size of mobe-le Sheden

dispative
als mic possel

Why care about x-ray diffraction of crystals?

Why should we care about x-rays, crystals, lattices, etc?

Metal Organic Frameworks

Porous frameworks for gas storage

Fundamental chemical bonding

Models for new catalysts

Organic 43%

Metal-Organic 57%

At least one transition metal. In, Tl, Ge, Sn, Pb, Sb, Bi, Po

Not Polymeric 89%

Single Component 56%

Multi Component 44%

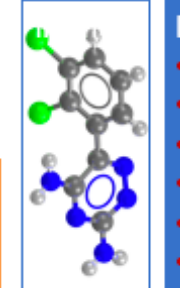
Organic

- Drugs
- Agrochemicals
- **Pigments**
- **Explosives**
- Protein ligands

Metal-Organic

Additional data

- >10,000 polymorph families
- >160,000 melting points
- >700,000 crystal colours
- >600,000 crystal shapes
- >23,000 bioactivity details
- >9,000 natural source data
- > 250,000 oxidation states

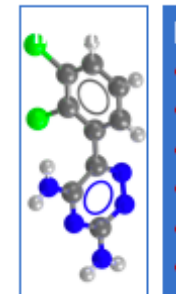


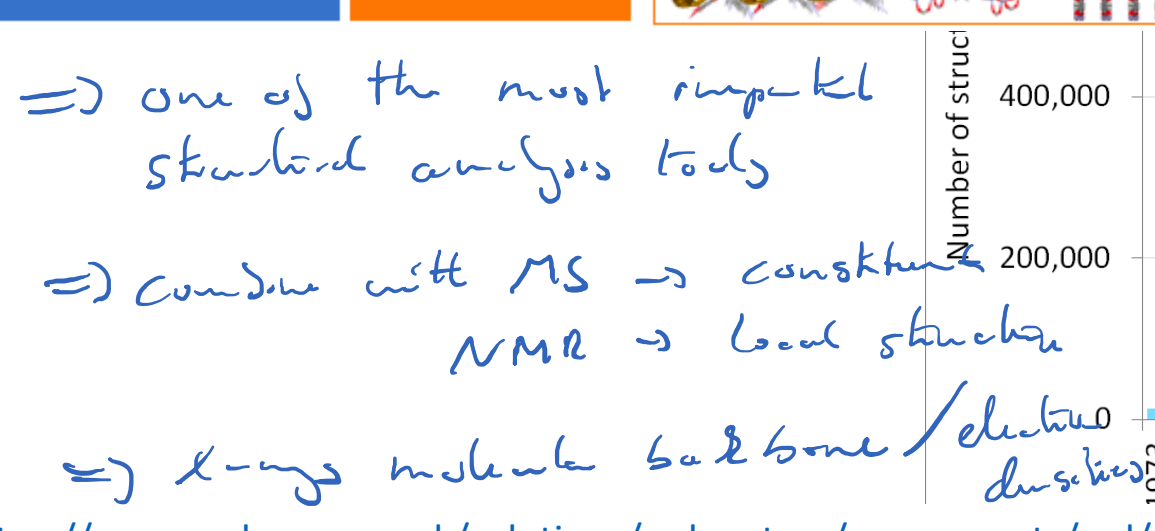
Links and subsets

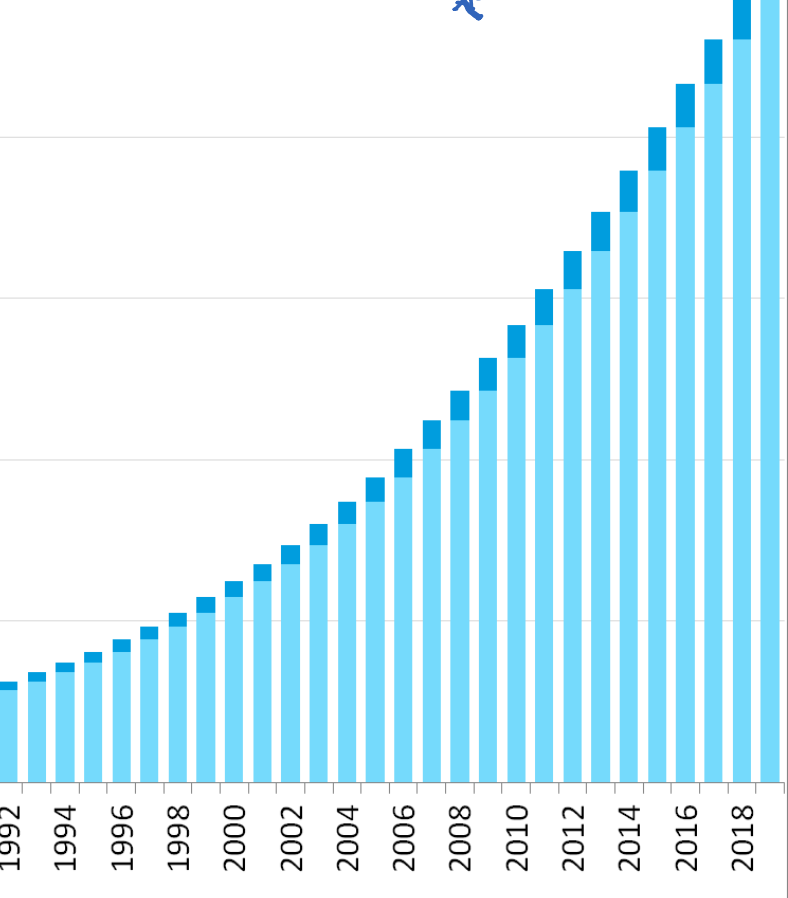
- Drugbank
- Druglike
- MOFs
- PDB ligands
- PubChem
- ChemSpider

1986

1984







Source:

Database (CSD)

The Cambridge Structural

https://www.ccdc.cam.ac.uk/solutions/csd-system/components/csd/

Year

Example: Diamondoids – Diamond Molecules

REPORT

Isolation and Structure of Higher Diamondoids, Nanometer-Sized Diamond Molecules

J. E. Dahl, S. G. Liu, R. M. K. Carlson*

+ See all authors and affiliations

Science 03 Jan 2003:

Vol. 299, Issue 5603, pp. 96-99 DOI: 10.1126/science.1078239

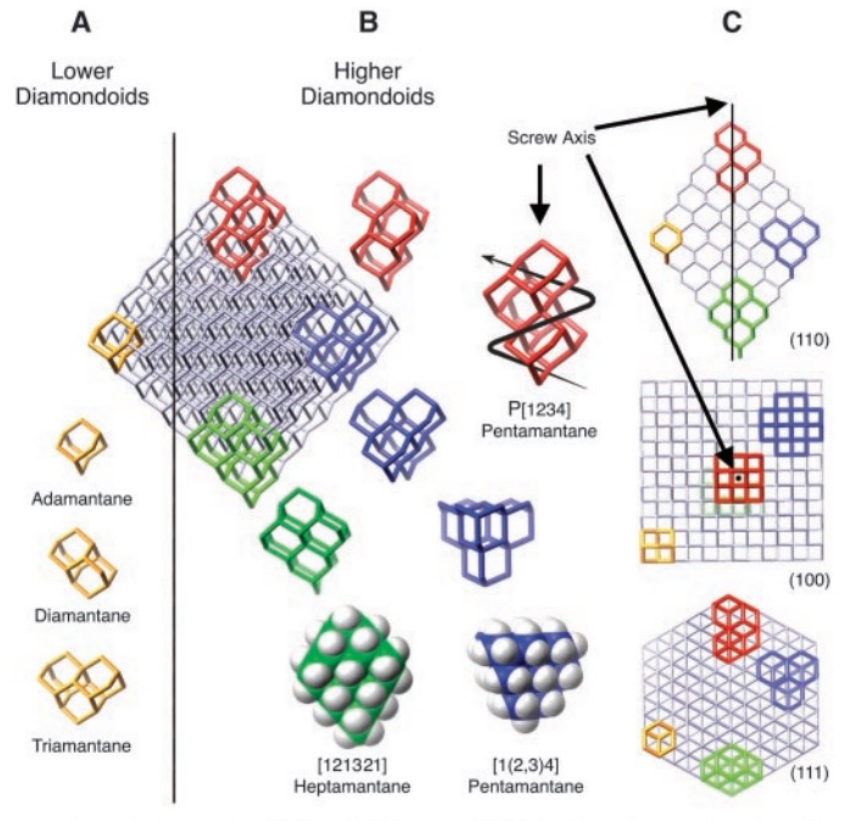
Example: déanne lois

Ouslie: horte tipue ont

that this is not just

another hydroconser

Fig. 1. The relation between the face-centered cubic diamond lattice and diamondoid structures. (A) Adamantane (yellow) is shown superimposed upon the lattice of a 455-carbon octaghedral diamond (some carbons removed for clarity). Adamantane, diamantane, and triamantane (all in yellow) are also shown separate from the diamond lattice. (B) Screwshaped higher diamondoid P [1234] pentamantane (red), pyramidal [1(2,3)4] pentamantane (blue), and rhombusshaped [121321] heptamantane (green) superimposed upon the diamond lattice and also separate from the lattice. (C) The 455-carbon diamond with superim-



posed diamondoid structures viewed along the (110), (100), and (111) lattice planes showing the diamond lattice faces of the pentamantanes and heptamantane. Views of the P [1234] pentamantane screw axis are indicated by straight arrows. The clockwise helical arrow indicates the groove in the red P [1234] pentamantane molecule.

Supplemental Material: Crystallization for XRD

Crystallization

We crystallized specific higher diamondoids from Hypercarb HPLC fractions by preparing super-saturated solutions in acetone. Crystallization vials (standard GC-MS autosampler vials) were sealed for approximately one to two weeks after which a small hole was made in the caps and the solvent allowed to evaporate. The crystals were harvested and submitted for structural determination by X-ray crystallography. Fig. S1

2

shows [1(2,3)4] pentamantane (structure $\underline{7}$ in Fig. 3 in the paper) grown using this method.

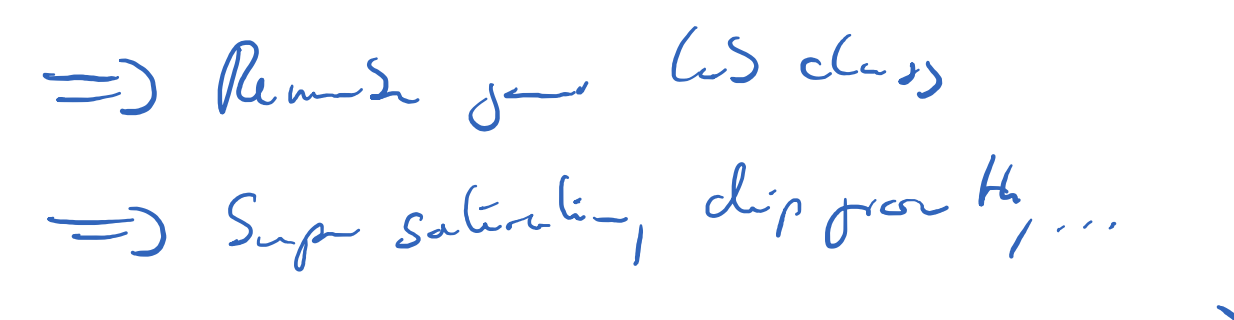
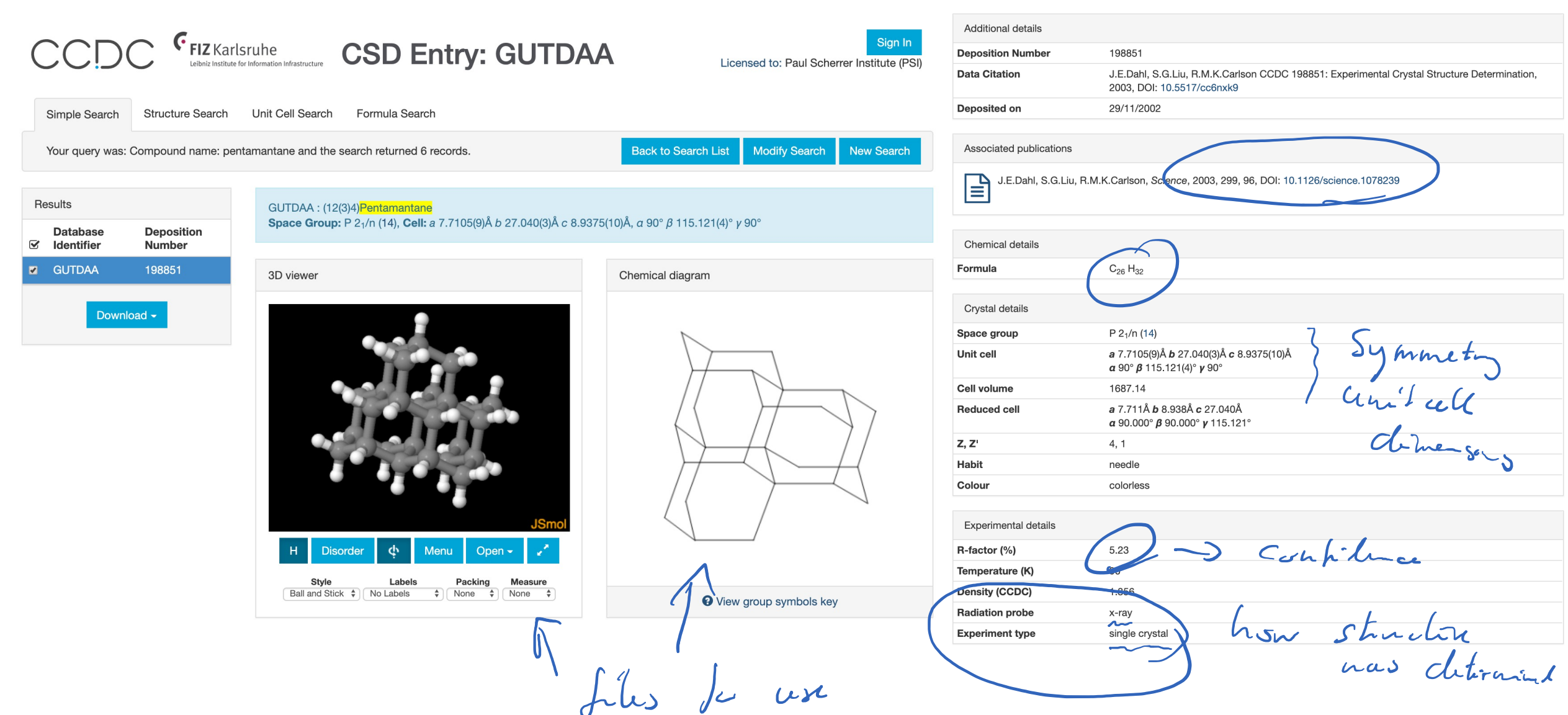




Fig. S1. Photomicrographs of [1(2,3)4] pentamantane crystals used for X-ray crystallography. Field of view, approx. 3.5 mm. Photograph, Marilyn Olmstead, U. C. Davis.

Ca appl 1-5 tehnions

Cambridge Structural Database entry

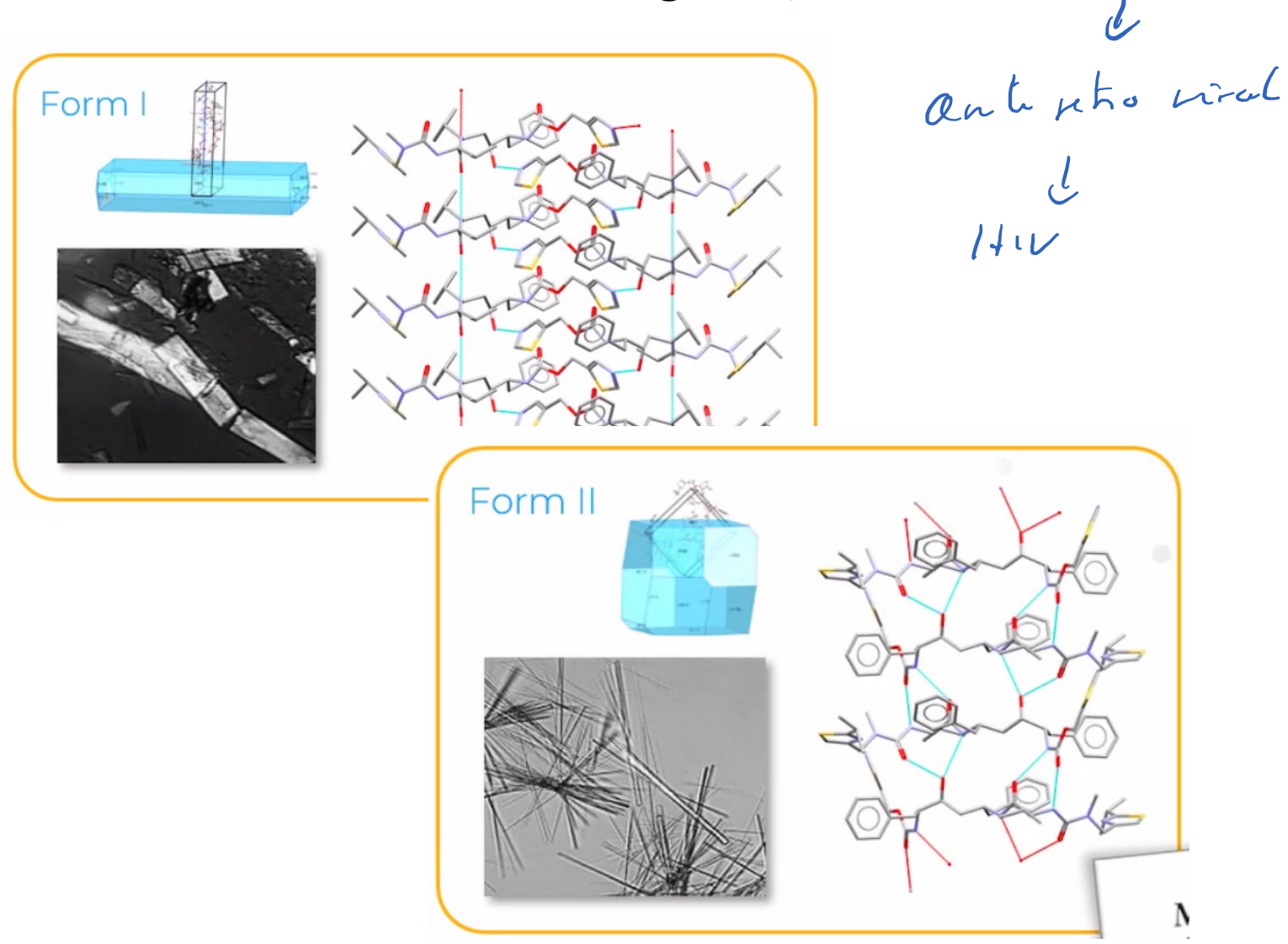


https://www.ccdc.cam.ac.uk/structures/Search?Compound=pentamantane&DatabaseToSearch=Published

A real world example: Crystal structure of the Novir Drug — Rifshowir

Crystalline structure of (drug) compounds determines

- Melting properties
- Hygroscopicity
- Hydrate formation
- Soluablility
- And other properites



A real world example: Crystal structure of the Novir Drug

Science news:

> Pharm Res. 2001 Jun;18(6):859-66. doi: 10.1023/a:1011052932607.

Ritonavir: an extraordinary example of conformational polymorphism

J Bauer ¹, S Spanton, R Henry, J Quick, W Dziki, W Porter, J Morris

Affiliations + expand

PMID: 11474792 DOI: 10.1023/a:1011052932607

Abstract

Purpose: In the summer of 1998, Norvir semi-solid capsules supplies were threatened as a result of a new much less soluble crystal form of ritonavir. This report provides characterization of the two polymorphs and the structures and hydrogen bonding network for each form.

Methods: Ritonavir polymorphism was investigated using solid state spectroscopy and microscopy techniques including solid state NMR, Near Infrared Spectroscopy, powder X-ray Diffraction and Single crystal X-ray. A sensitive seed detection test was developed.

Results: Ritonavir polymorphs were thoroughly characterized and the structures determined. An unusual conformation was found for form II that results in a strong hydrogen bonding network A possible mechanism for heterogeneous nucleation of form II was investigated.

Conclusions: Ritonavir was found to exhibit conformational polymorphism with two unique crystal lattices having significantly different solubility properties. Although the polymorph (form II) corresponding to the "cis" conformation is a more stable packing arrangement, nucleation, even in the presence of form II seeds, is energetically unfavored except in highly supersaturated solutions. The coincidence of a highly supersaturated solution and a probable heterogeneous nucleation by a degradation product resulted in the sudden appearance of the more stable form II polymorph.

Similar articles

Business news:



Abbott Reports Production Problems For Norvir

27-07-1998

Abbott Laboratories has reported that it is having difficultiesmaintaining production of its HIV protease inhibitor Norvir (ritonavir). The problems are related to its capsule formulation of the antiretroviral.

"We have encountered an undesired formation of a Norvir crystalline structure that affects how the capsule form of Norvir dissolves," commented Arthur Higgins, senior vice president for pharmaceutical operations at Abbott. Although the problem has been identified, to date the company has been unable to come up with a solution.

Abbott stressed that capsules already in circulation are not affected, but there will be shortages and an interruption in supply of the product. Given the seriousness of interrupting treatment in highly-active antiretroviral therapy (which could be associated with the development of resistance and ultimately treatment failure), Abbott is planning to manufacture Norvir in a substitute oral solution so that patients on the drug can maintain their supply. It is estimated that 60,000-70,000 people with HIV are taking the drug.

Effect On Full-Year Sales? Abbott had been projecting sales of around \$250 million for Norvir in 1998, and as yet it is unclear whether the supply problems will impact this figure. Sales of the drug last year were around \$170 million, less than the performance seen with the other protease inhibitors in 1997. Datamonitor says that Merck & Co's Crixivan (indinavir) had sales of \$240 million last year, while Agouron's Viracept (nelfinavir) made around \$190 million last year, and Roche's Invirase (saquinavir) made over \$200 million.

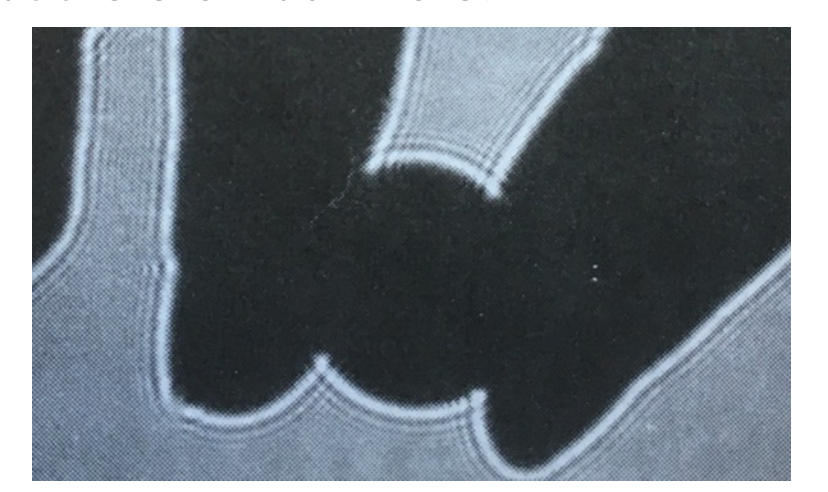
Analyst Hemant Shah of HKS & Co told Reuters that the other protease inhibitors would definitely gain market share at the expense of Norvir, adding that the impact on Abbott's bottom line will depend greatly on the duration of the problem.

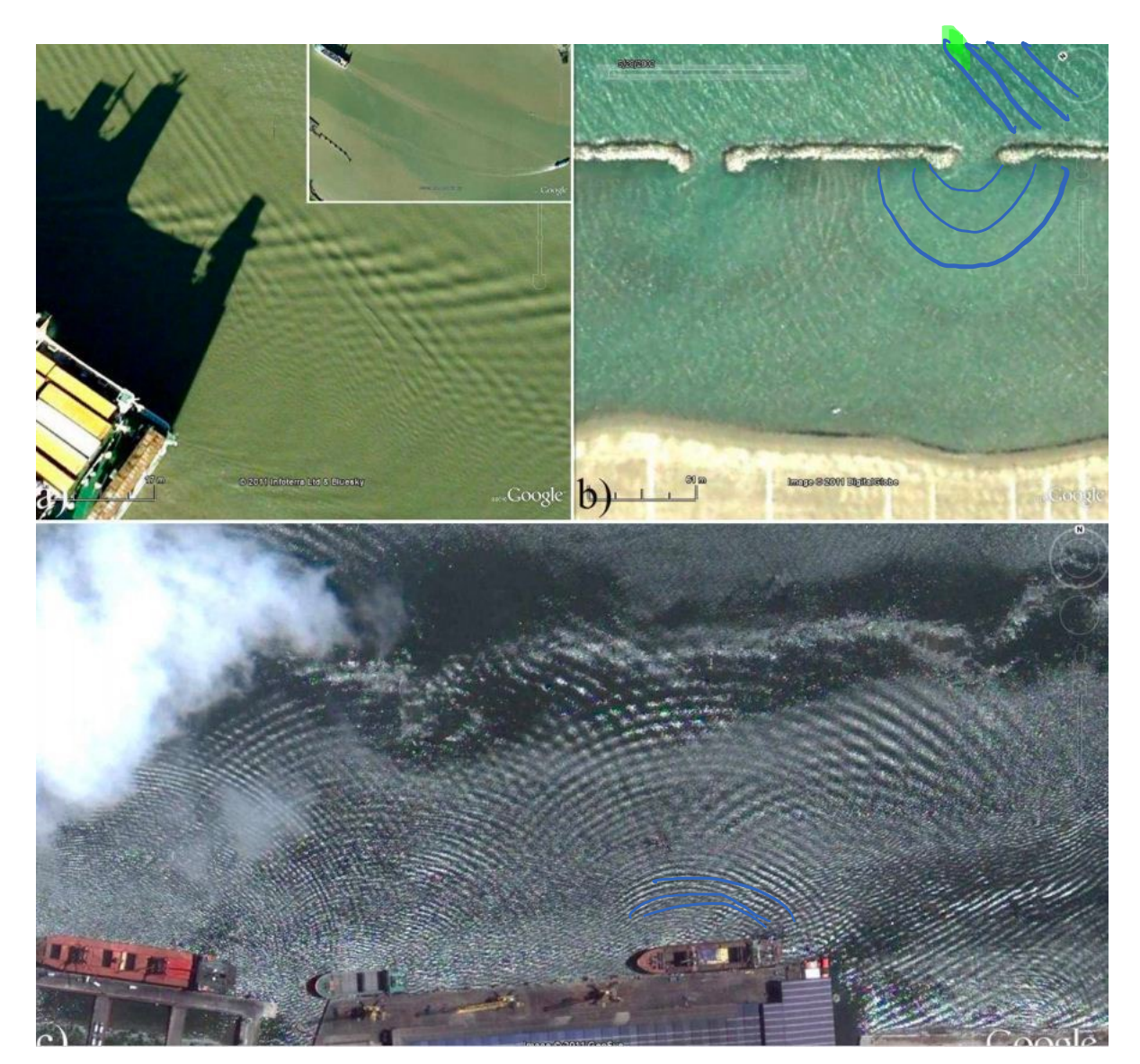
Some very basics about diffraction and scattering

https://physicsforme.com/2012/01/04/teaching-waves-with-google-earth/

Diffraction, a short review

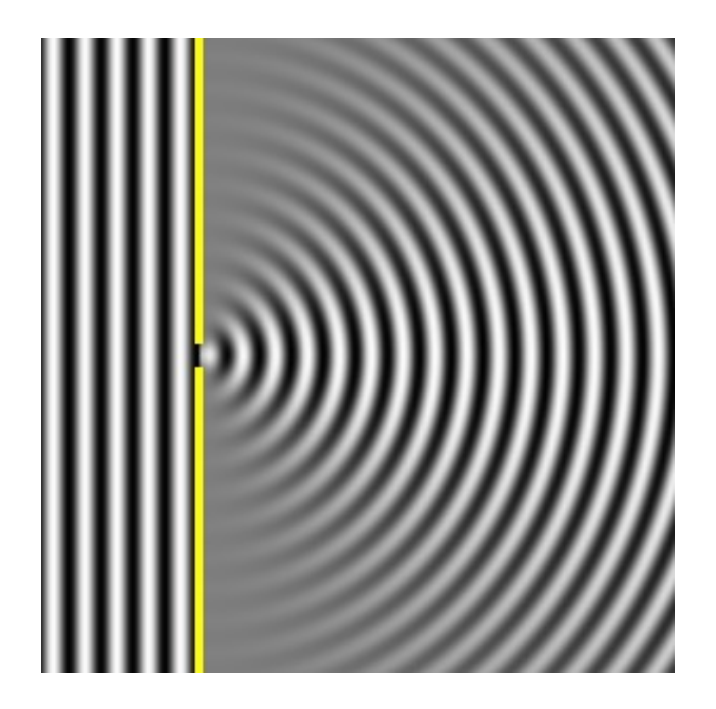
- Should be familiar concept
- A wave encountering an object changes its wavefront. Note that this can also be a density change (later more)
- Fundamental properties of all waves with relevant effects from electron microscopy to shaping coastal landscapes
- In optics most commonly known for limiting resolution in optical setups (microscopes)
- But there is much more!

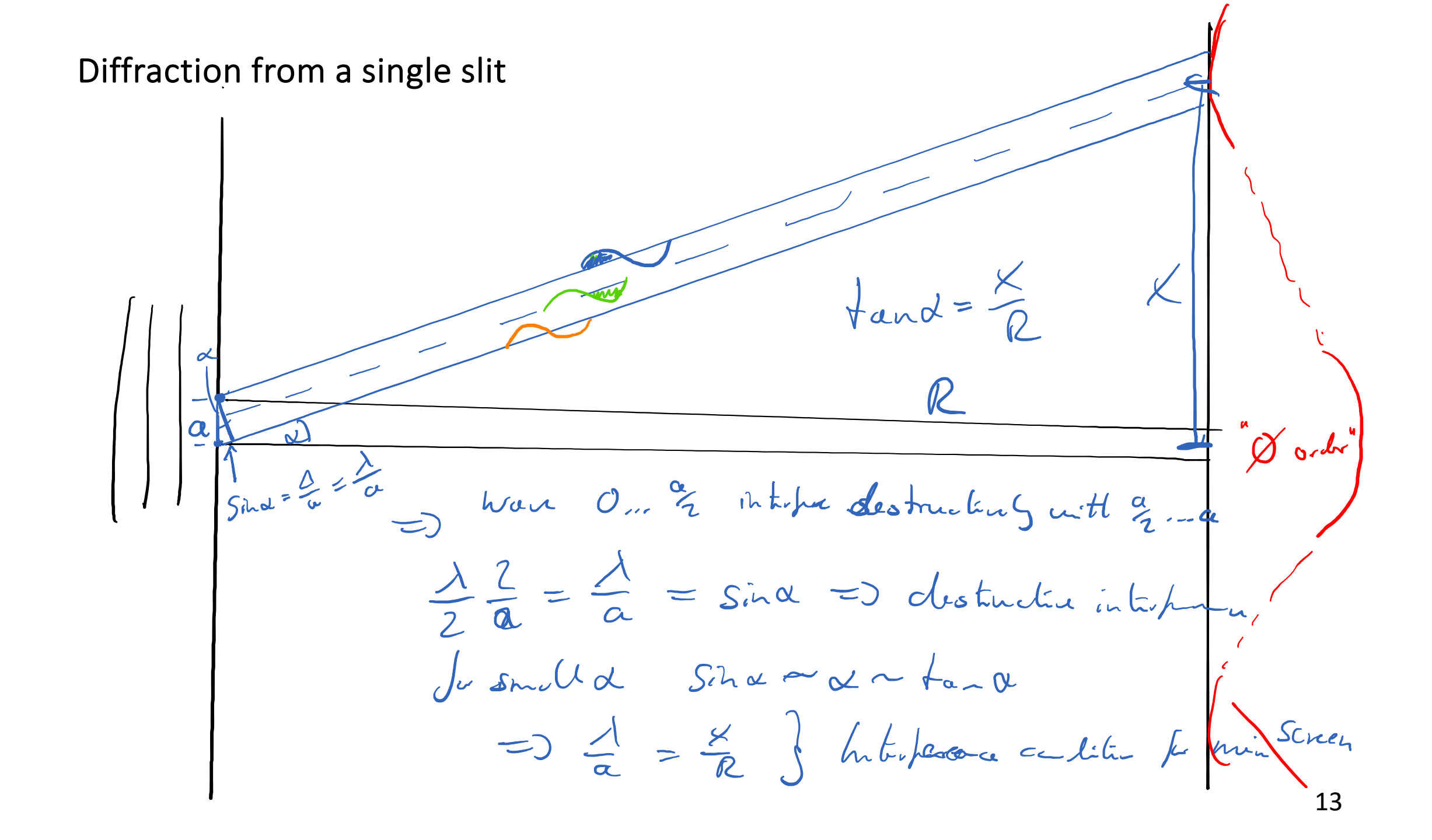




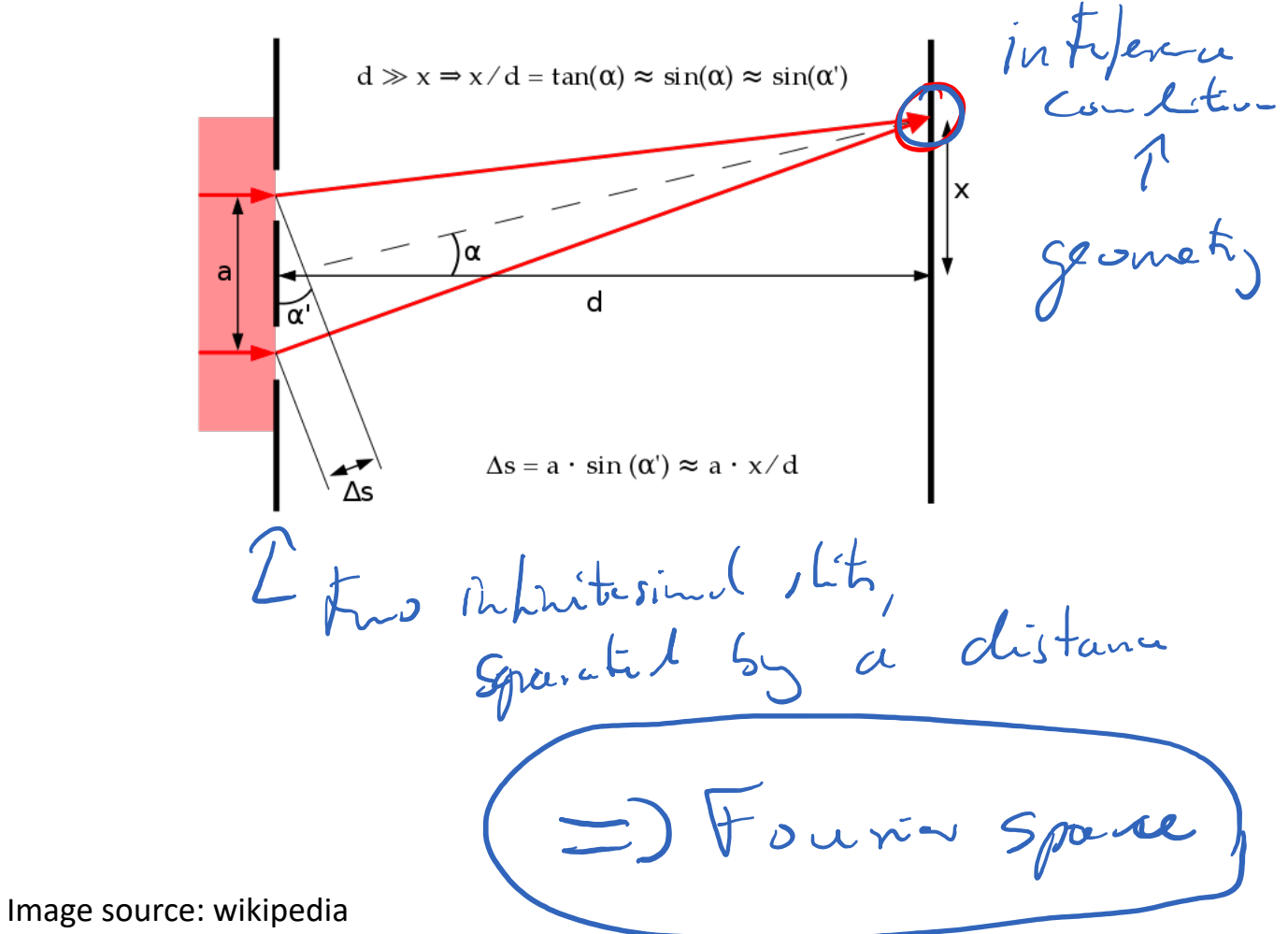
The Huygens-Fresnel Principle

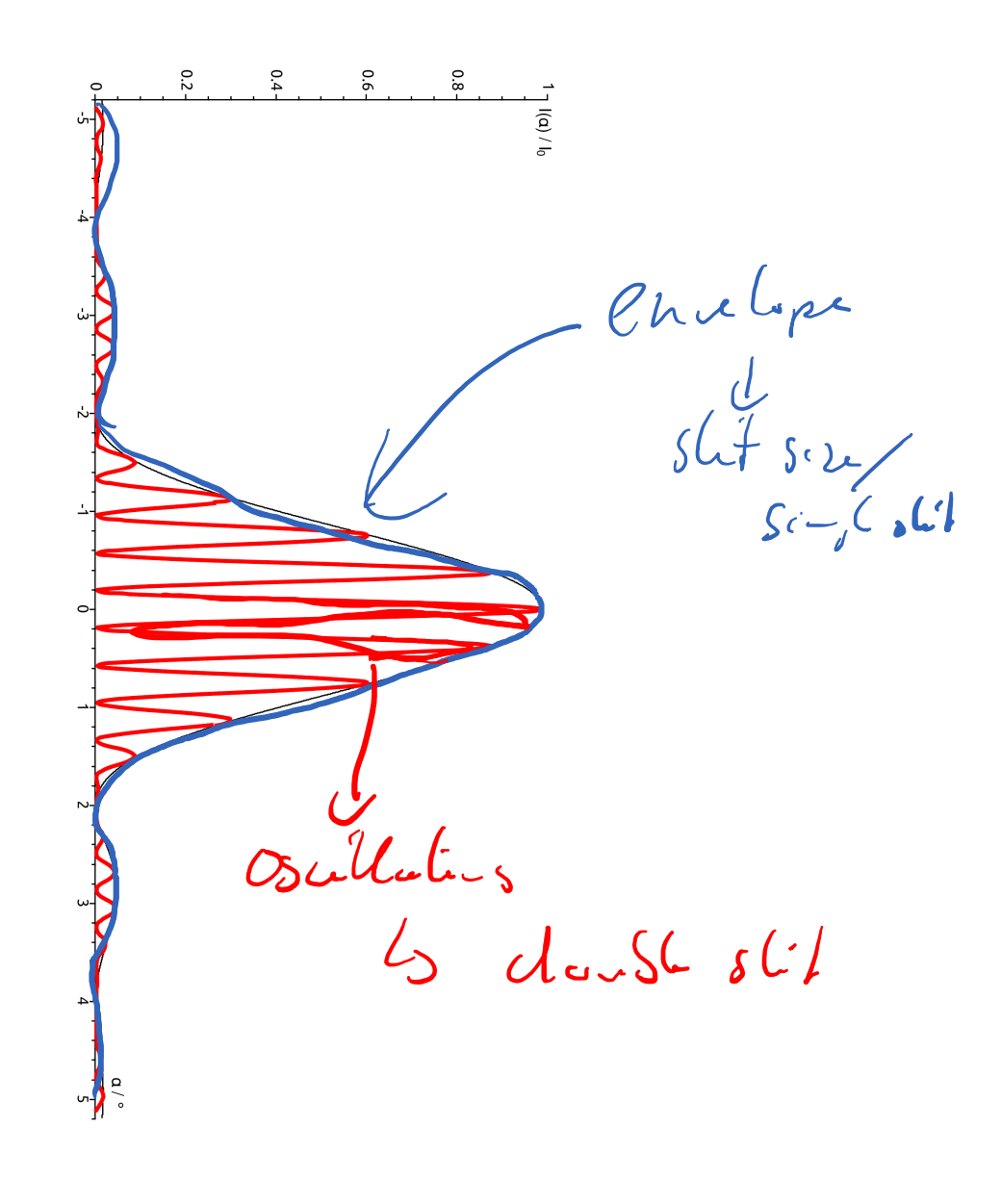
- Hugens: every point a wave (a luminous disturbance) reaches becomes a source of a spherical wave; the sum of these secondary waves determines the form of the wave at any subsequent time.
- Huygens-Fresnel: every unobstructed point of a wavefront serves as a source of spherical secondary wavelets. The amplitude of the wave beyond is the superposition of all these wavelets. (includes amplitude and relative phase)





The double slit





14

Diffraction examples

Sufy

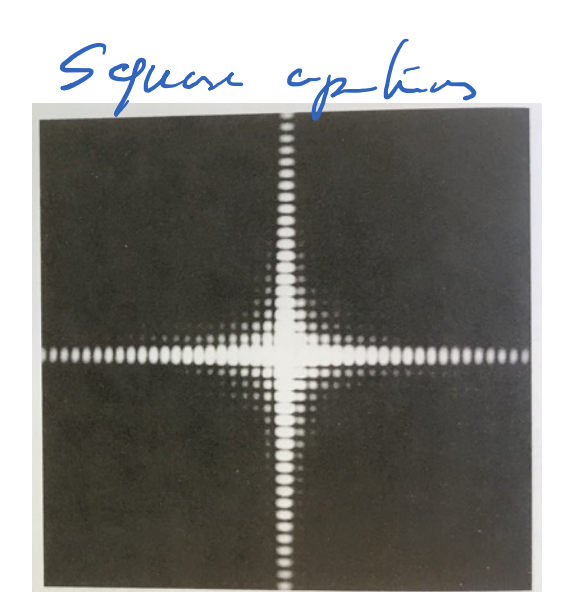
w=50μ d=150μ 3 slits 4 slits 5 slits 7 slits

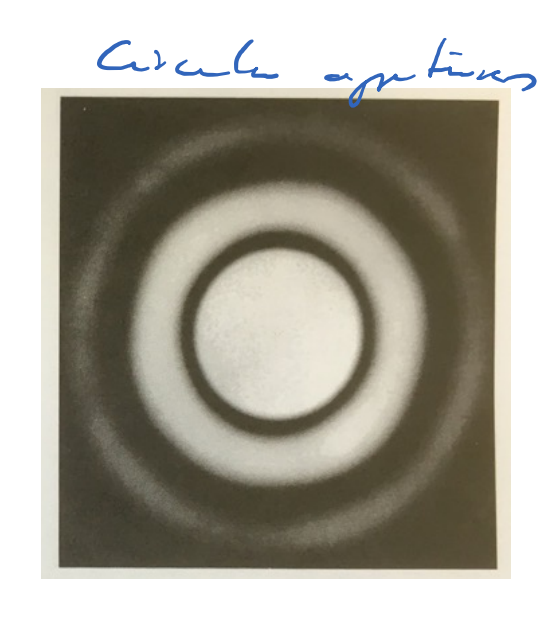
1 slit

2 slits

4 slits

5 slits





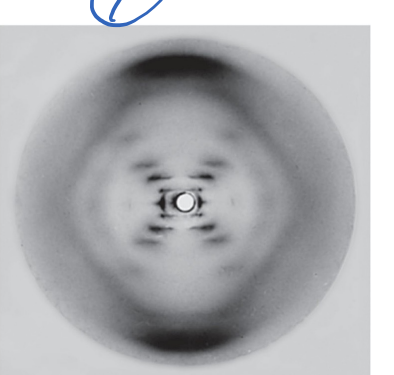
Again Scatty approved
our cours
nowlike limit
of delects

Watsa Cil Rosalin Frakkin

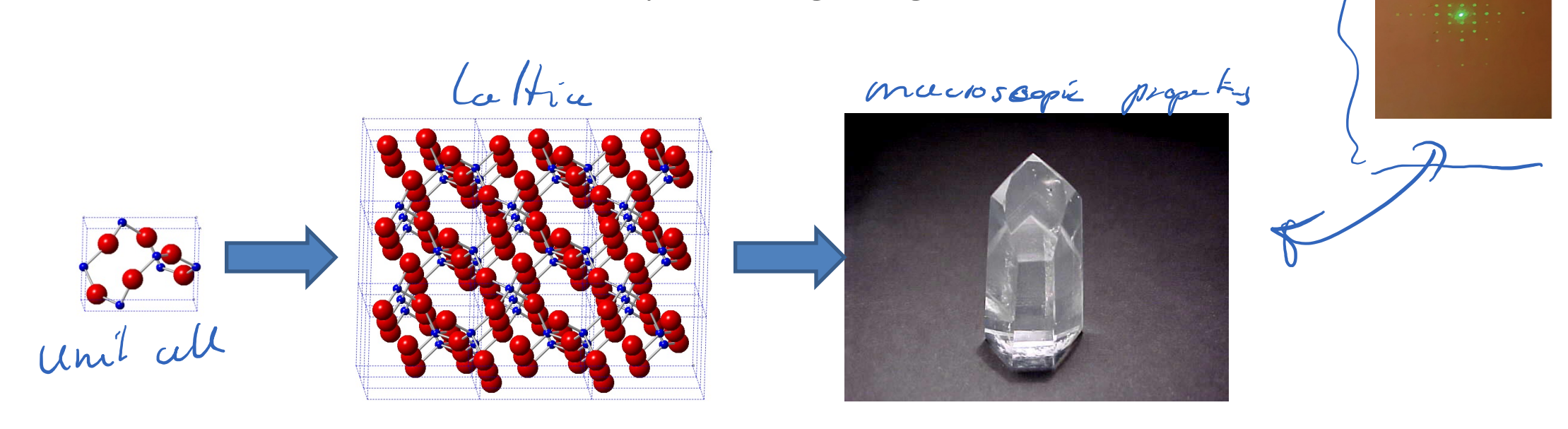


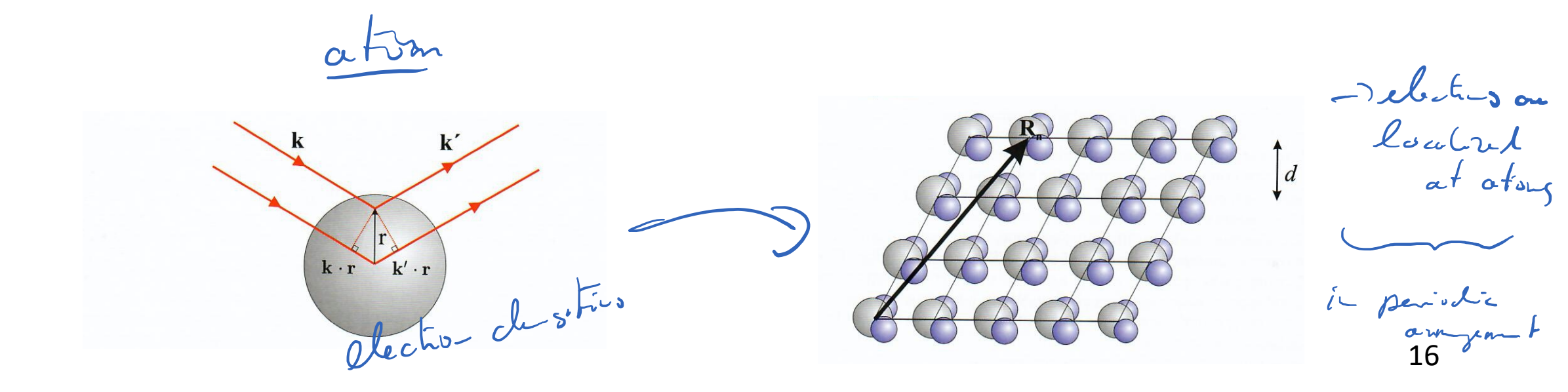


Land Silva

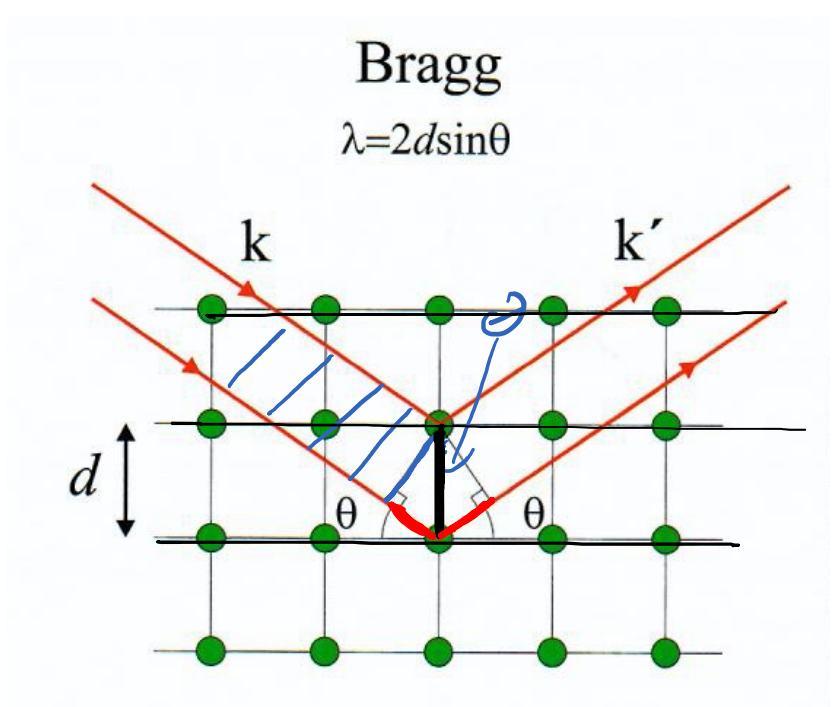


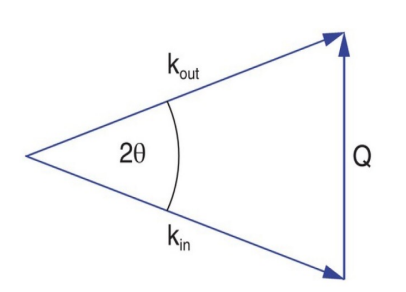
Crystaline materials are characterized by the long-range order





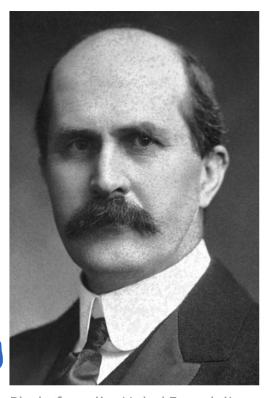
Bragg scattering





-) atoms i-definel

from these planes



Sir William Henry

Bragg Prize share: 1/2

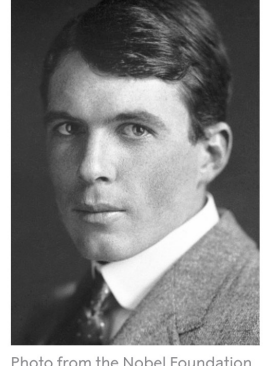


Photo from the Nobel Foundation William Lawrence

Bragg

Prize share: 1/2

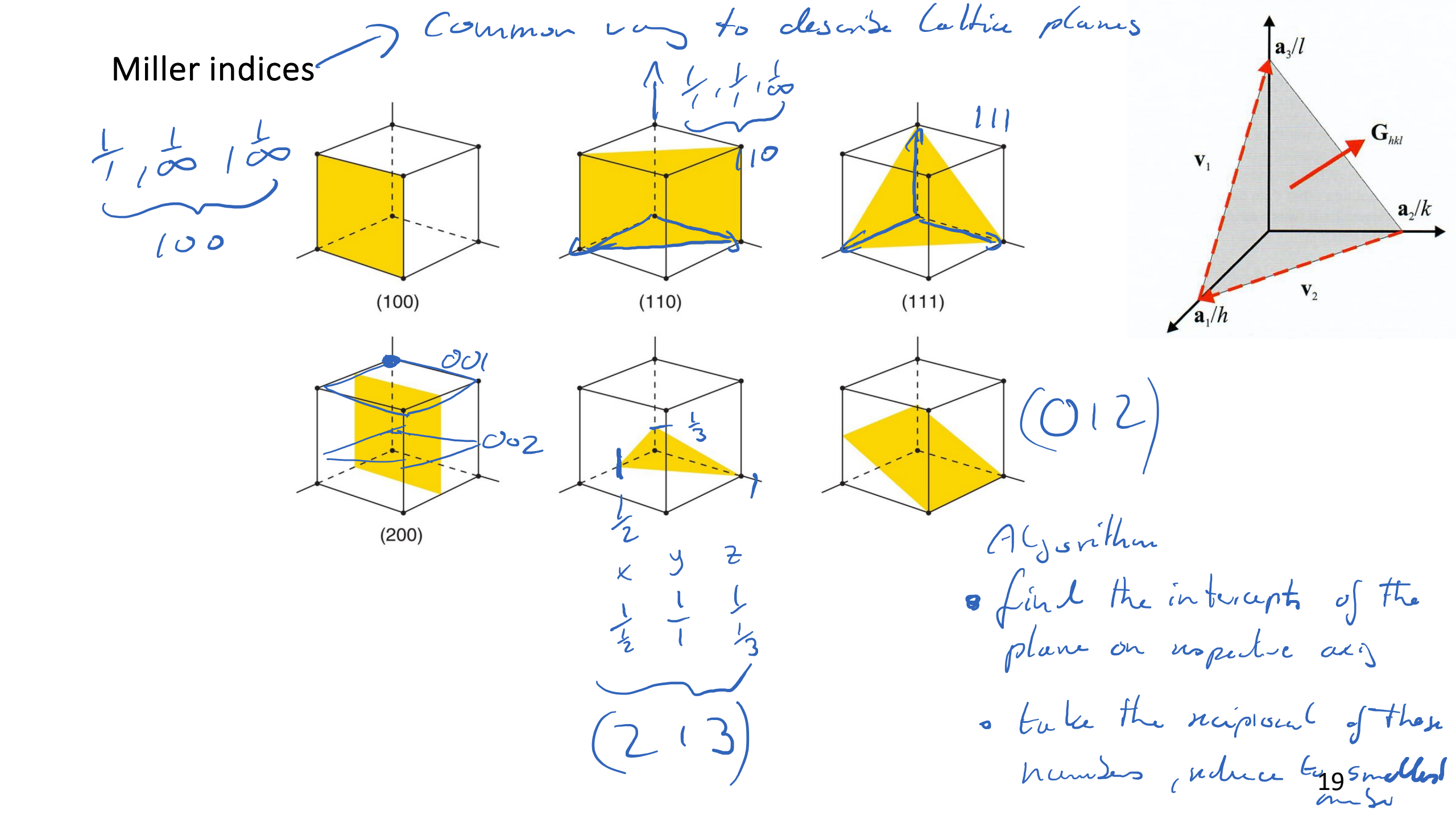
Main idea : exploit interfer e phenomena Constructive in Future e $\lambda = 2 \cdot d \sin \theta$

$$Sin \Theta = \frac{n \Lambda}{2 \Lambda} \Rightarrow 2 d sin \Theta = n \Lambda$$

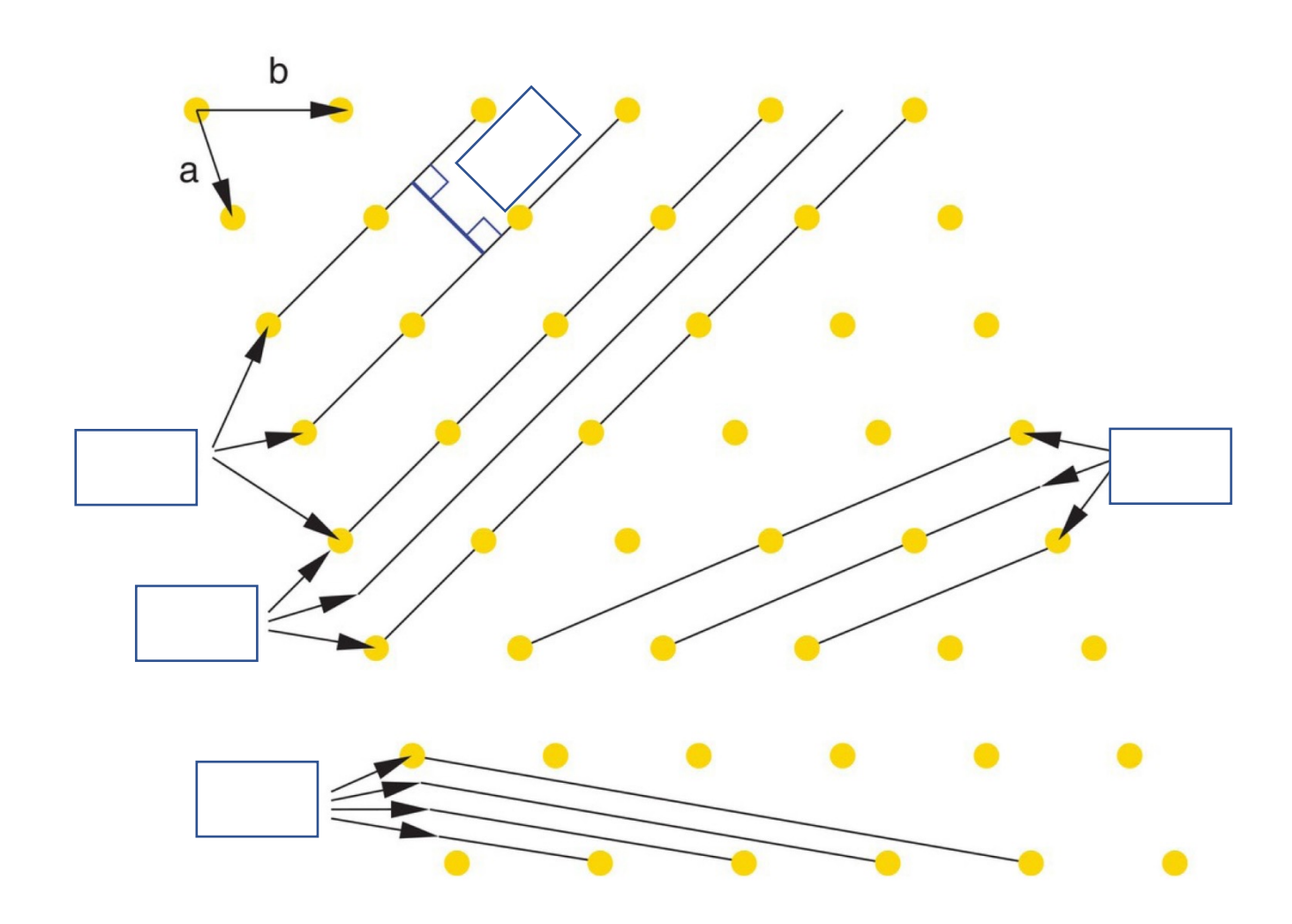
n= 1,2,3,---

13 ray 6217

Journal way of cleanising Cothin plans Lattice planes 1) Look where plane intersect axis Bragg 2) lake the inverse nude & relied to smalled (10) planes (21) planes Stip () an interest in 00 az, interest in 1 Step 1: a, interests at 2 az interects at 1 Step (2) is - 1 Step 2: 1/2 = 1 2/18

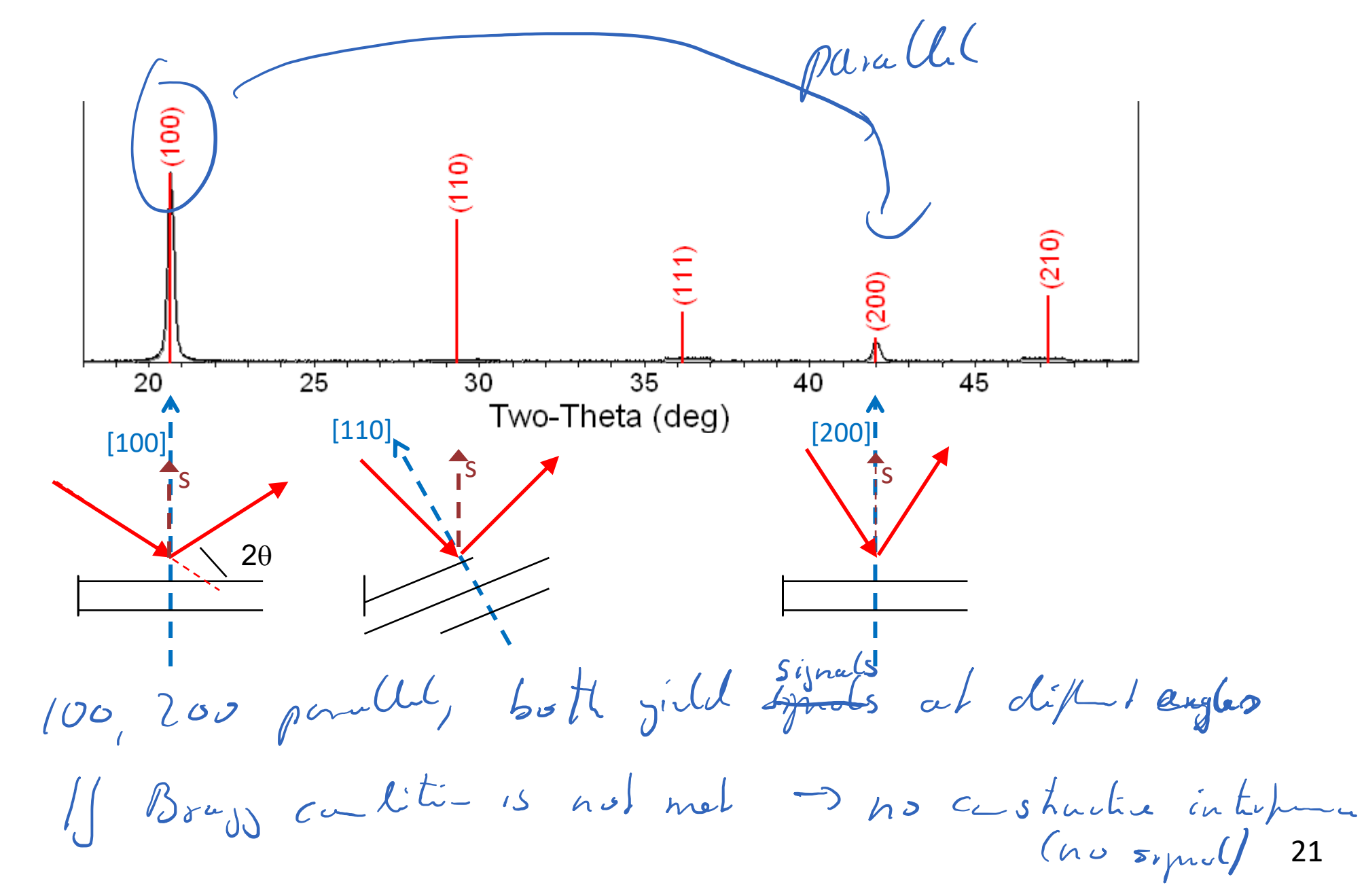


Exercise: Identify lattice planes



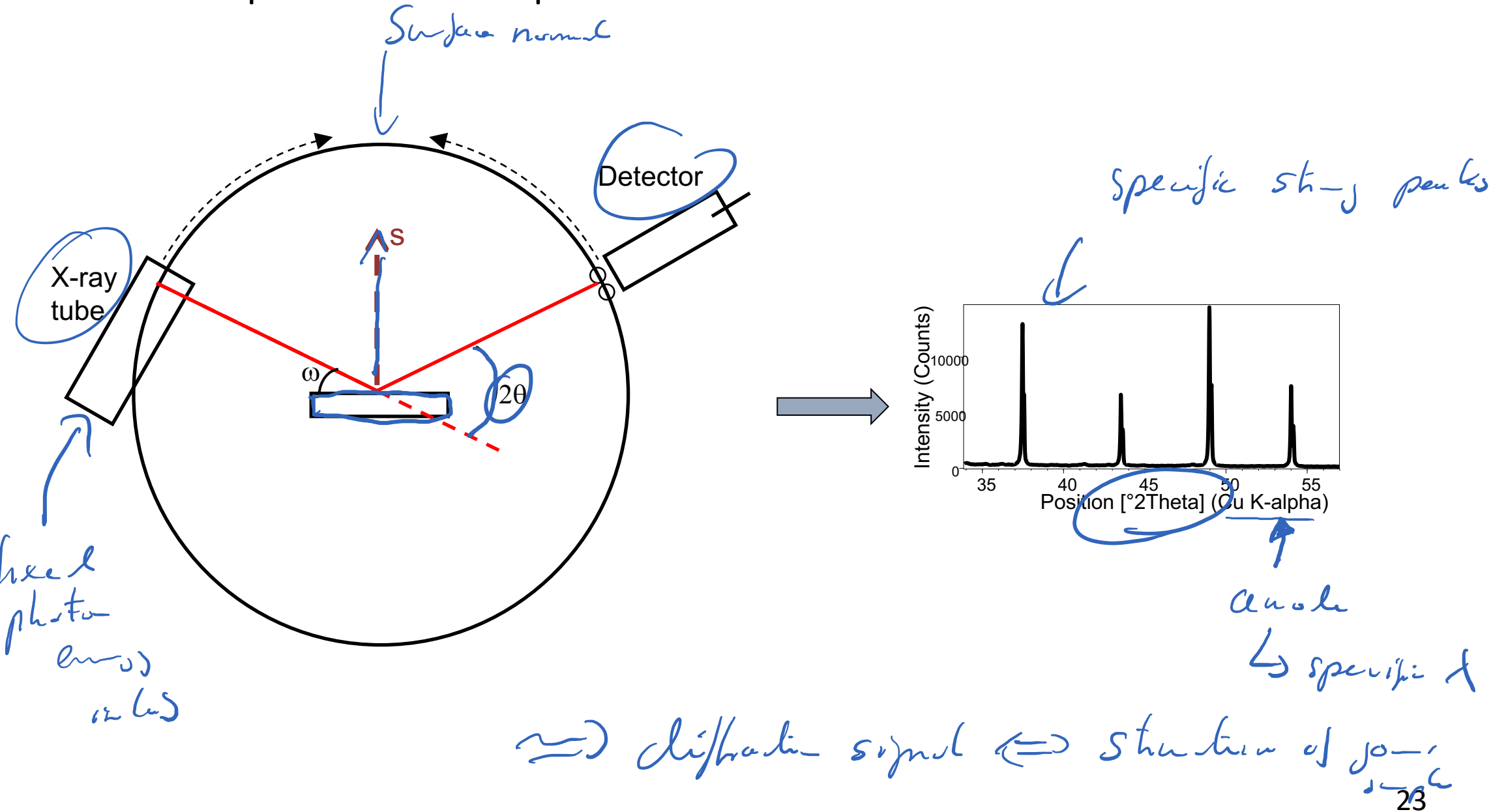
A single crystal (typically) produces one family of Bragg peaks for fixed geometry

and λ

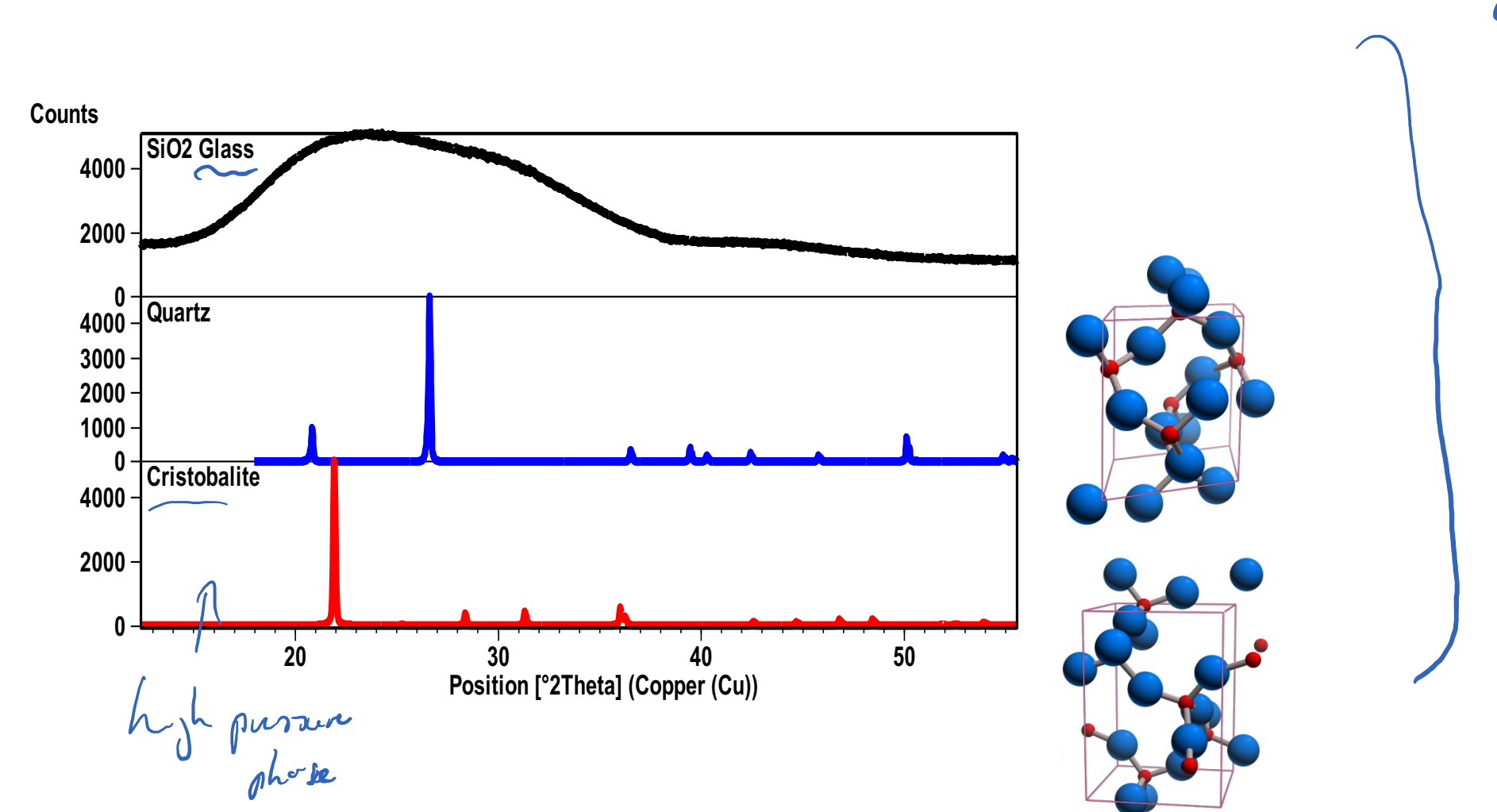


Diffraction examples

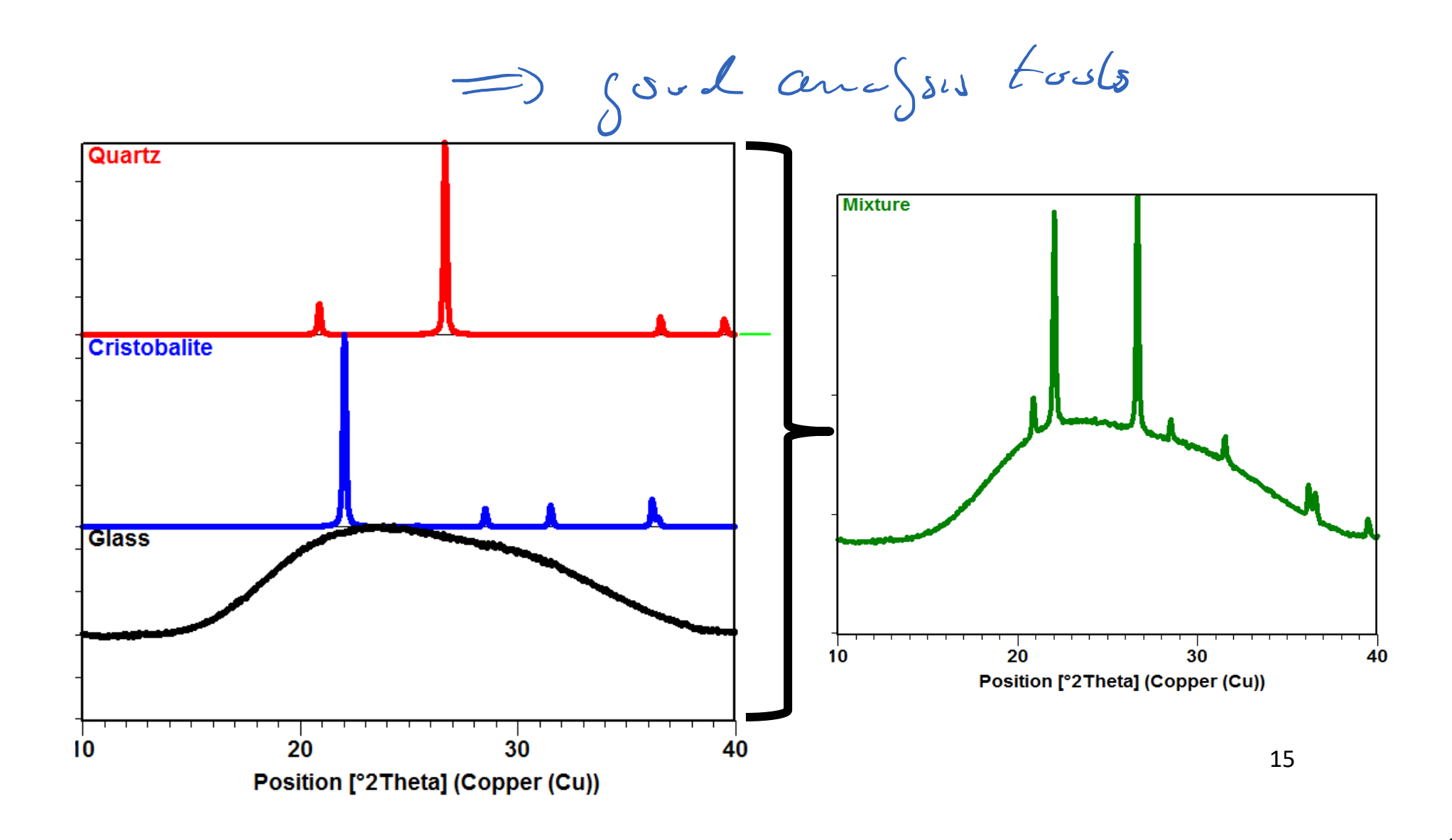
Diffraction experiment - example



Characteristic signals from different – chemically identical – samples

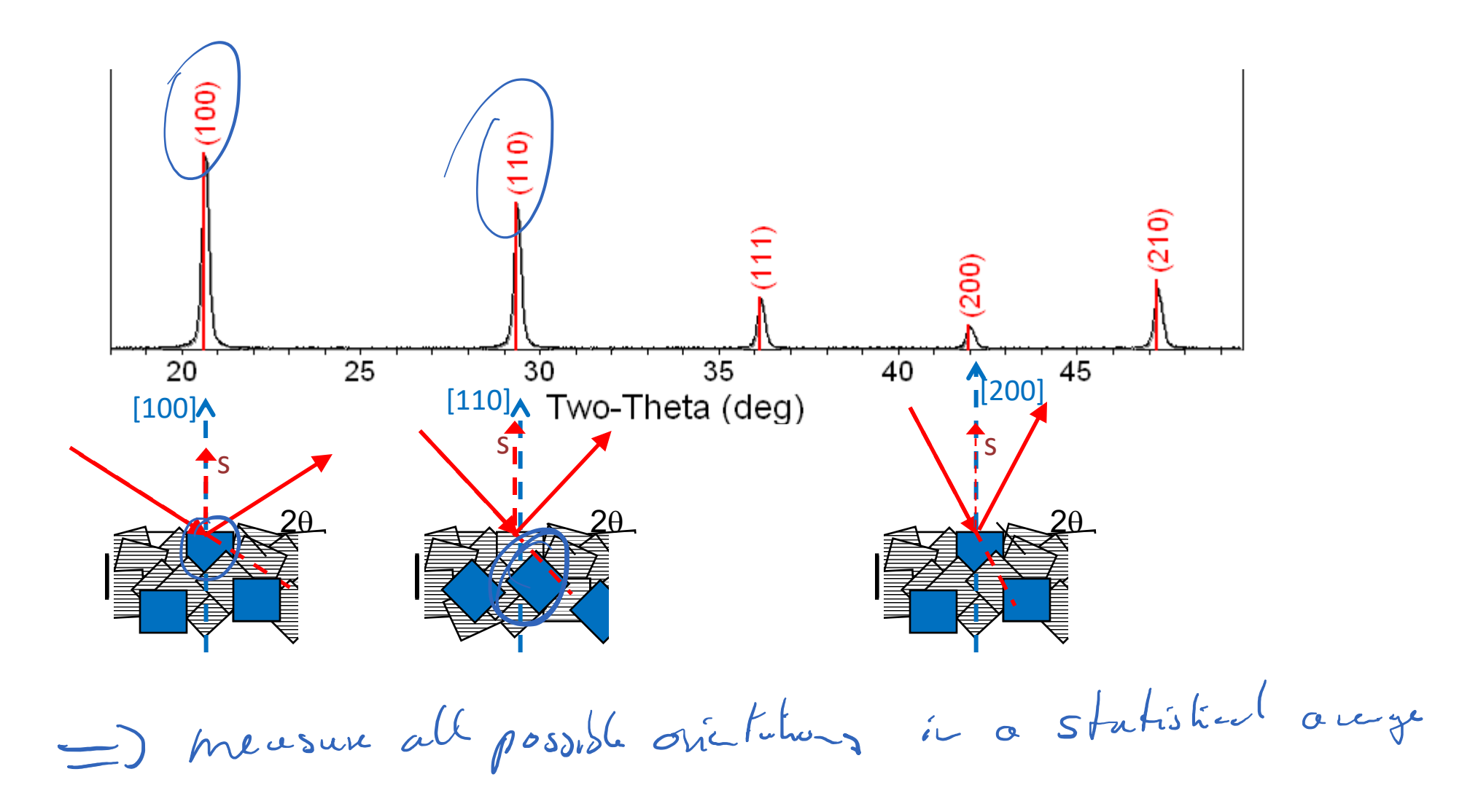


all SiO25-pa all shucking but their structure different The diffraction pattern of a mixture is a simple sum from each component phase

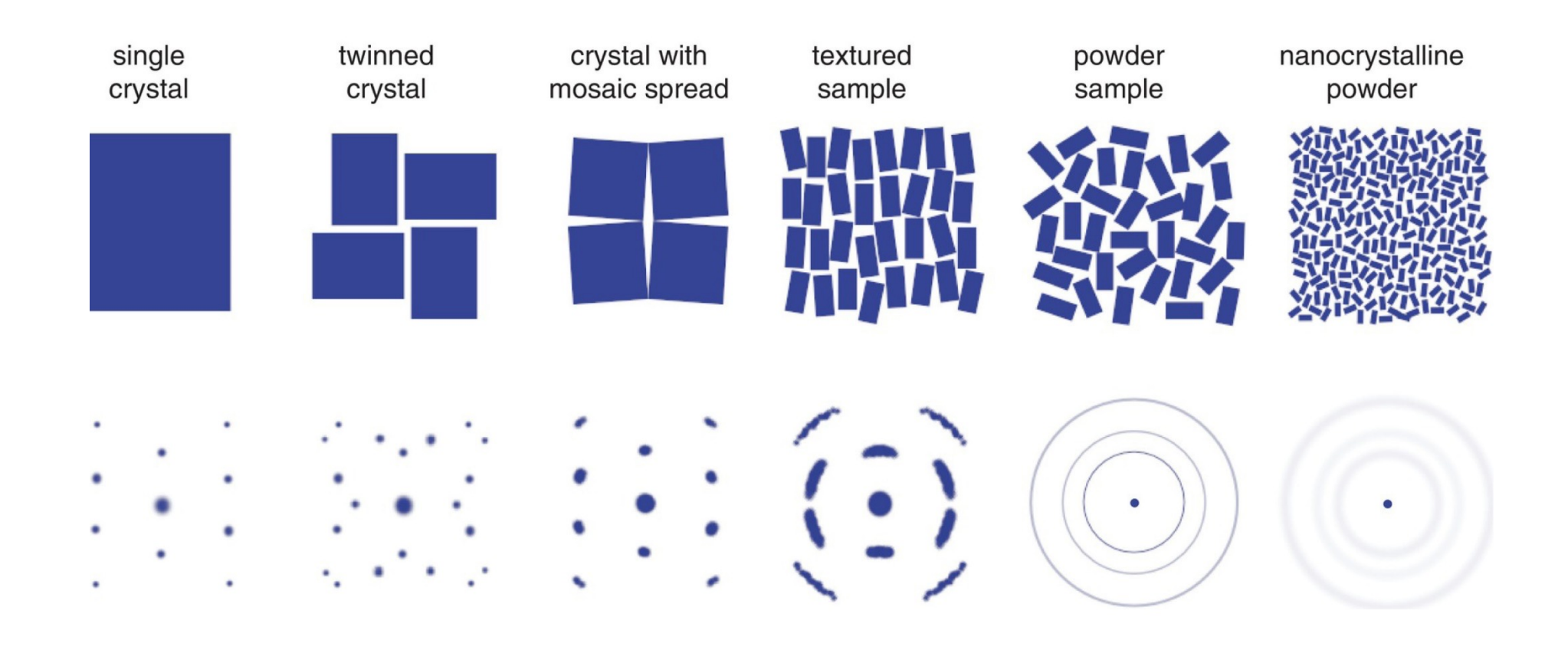


Powder diffraction

Diffraction of a polycrystalline sample



Diffraction signal of different sample types



Powder diffraction experiments 20 de talor Coptullites = 20 pixel de tectors Brow anyles -> powder yields ration ange - 20

Powder diffraction geometry — Laue diffraction



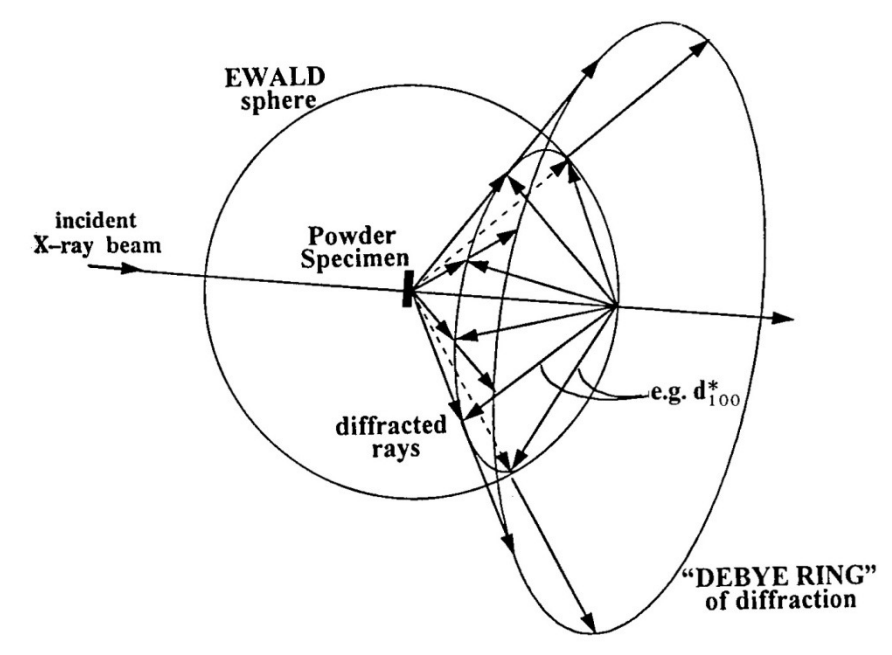
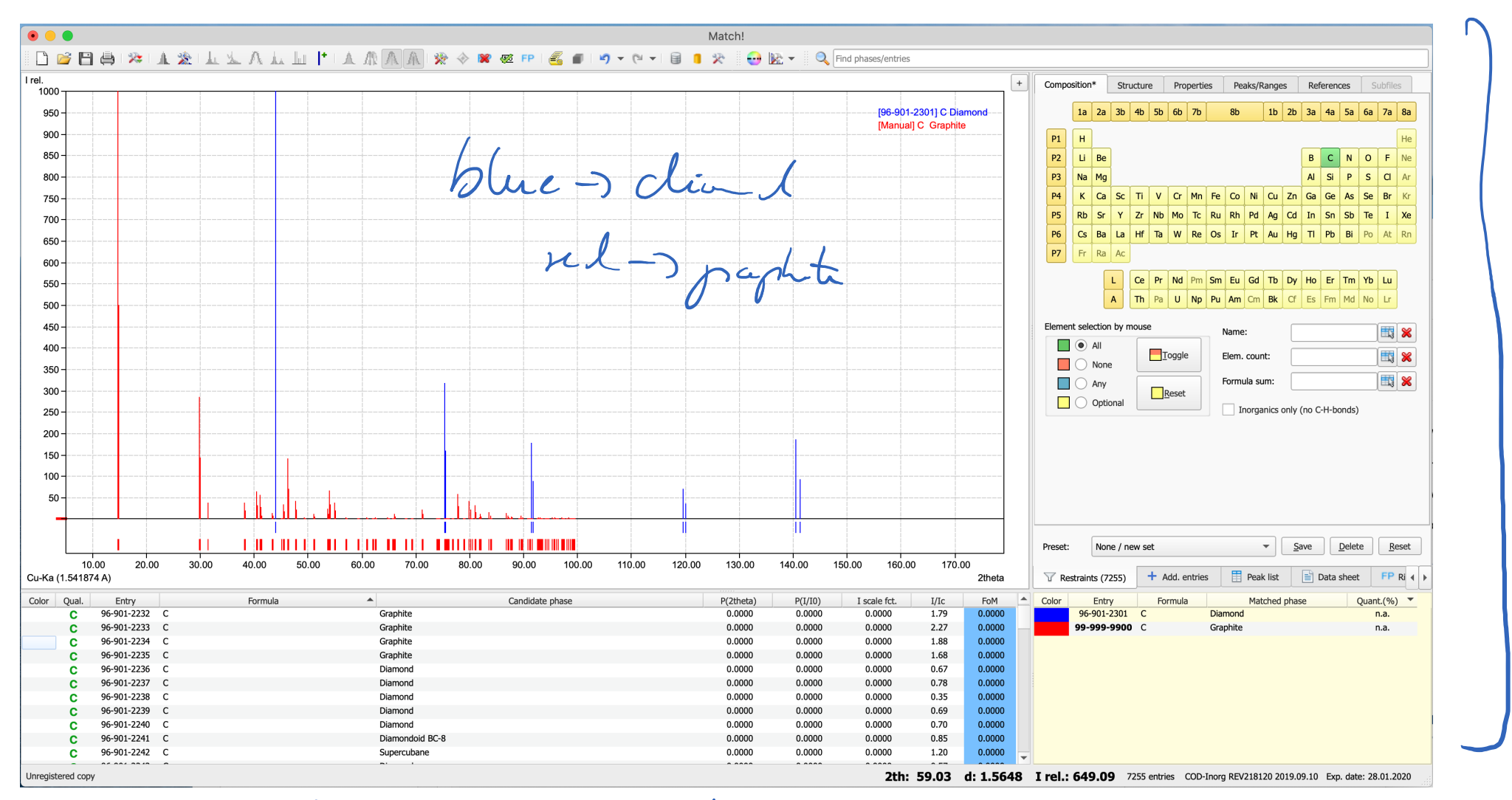


Figure 3.9. The intersection of d_{100}^* vectors from a powder with the Ewald sphere.

I transmission gesmet Drings in delictor plane Dearlie strip/film detector, tody 20 piece detector

Two-Theta (dec)

Powder diffraction data bases for elemental analysis



Ja Structucal

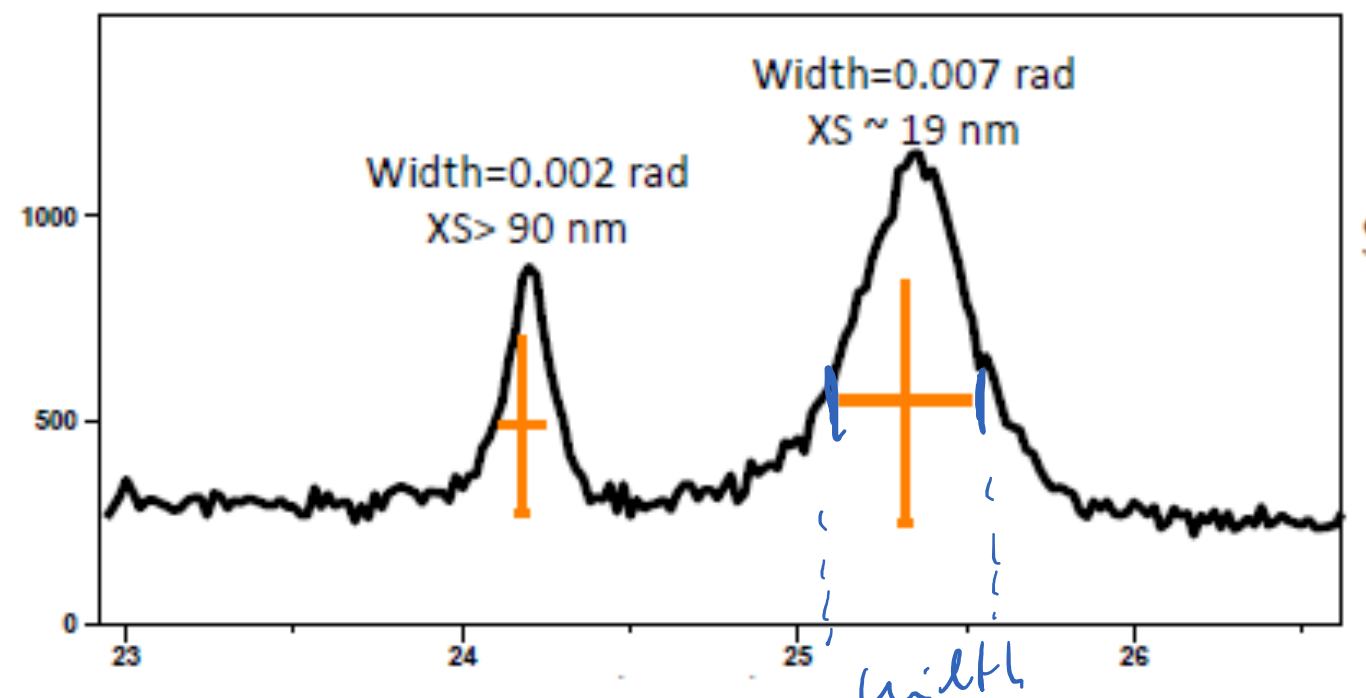
Phase and Jos

fud in your pattern, -> spits out shutur

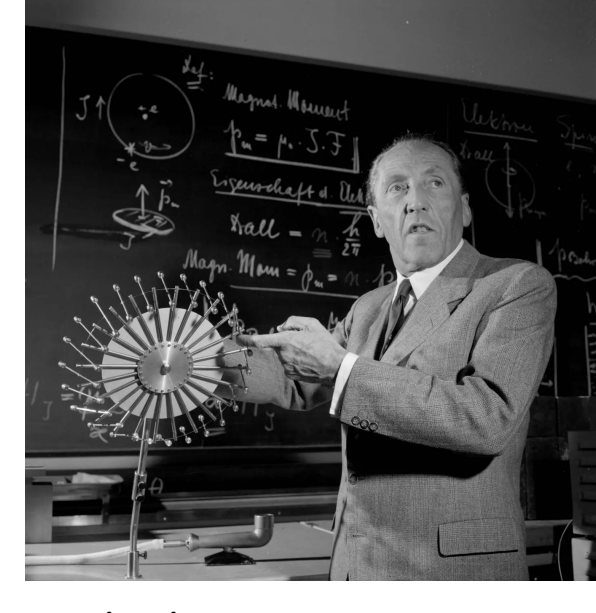
Debye-Scherrer Formula

The diffraction peak width may contain microstructural

information



 $royhy = \frac{100m}{100m}$ $Size = \frac{K}{Width*cos \theta}$



Paul Scherrer Swiss Physicist (1890-1969)

Relation with of diffraction peak weith particle size

Jor small 5-ples with-t inherita
translation of symmetry
32

Exercise: Colloidal nanoparticles

The diffraction experiments were carried out with a Stoe STADI-P X-ray powder diffractometer at University College London with a Ge(111) monochromator before the sample. A Cu $K\alpha_1$ X-ray beam of wavelength 0.154056 nm was used. The samples were measured in 0.35 mm diameter glass capillaries at room temperature. Capillary diameters were checked to be equal with a micrometer. The diffraction patterns were collected using a position-sensitive

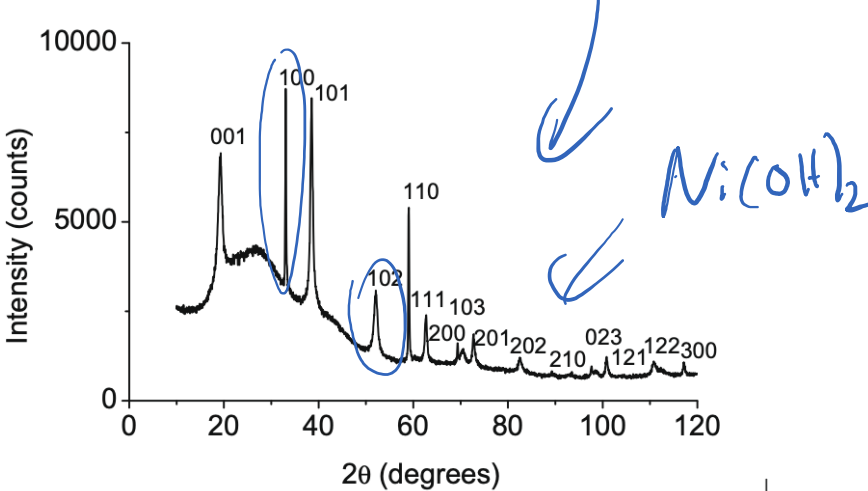


Fig. 1. X-ray diffraction pattern from Ni(OH)₂ dispersion c = 4.610(3) Å) with diffraction peaks labeled with hkl indice

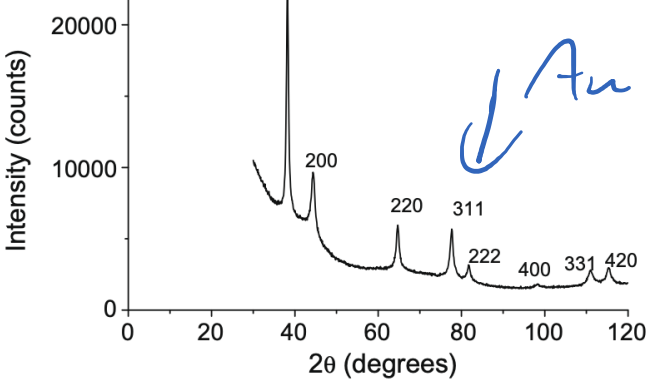


Fig. 2. X-ray diffraction patterns from dispersed Au particles (a = 4.067(3) Å) with diffraction peaks are labeled with hkl indices.

Contents lists available at ScienceDirect

Journal of Colloid and Interface Science

www.elsevier.com/locate/jcis



Use of wide-angle X-ray diffraction to measure shape and size of dispersed colloidal particles

S. Junaid S. Qazi a,*, Adrian R. Rennie , Jeremy K. Cockcroft , Martin Vickers b

Table 1 Results from the pseudo-Voigt function fit to the Ni(OH)₂ sample. 2θ is the peak position for the Cu K α_1 radiation wavelength (0.154056 nm).

hkl	Bragg angle 2θ (°)	Peak width 'β' (°)	Instrument resolution (°)	Corrected β (°)
001	19.25	1.140	0.121	1.02
100	33.06	0.197	0.115	0.08
101	38.52	0.593	0.114	0.48
102	52.06	0.876	0.117	0.76
110	59.05	0.248	0.120	0.13
111	62.67	0.550	0.122	0.43

Table 2Results from the pseudo-Voigt fit to the Au particles. 2θ is the peak position for the Cu K α_1 radiation wavelength (0.154056 nm).

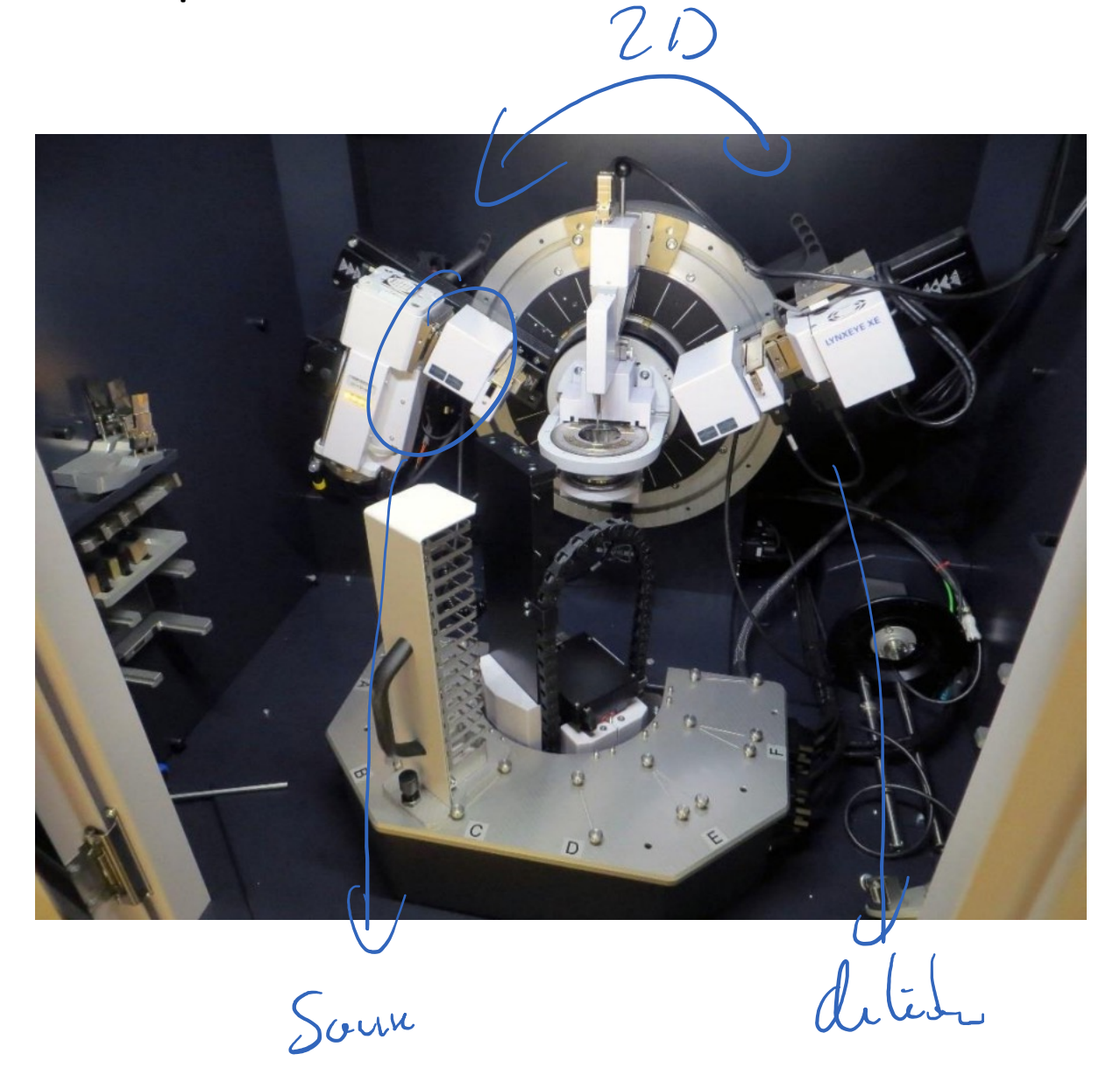
hkl	Bragg angle 2θ (°)	Peak width 'β' (°)	Instrument / resolution (°)	Corrected β (°)	
111 200 220 311	38.21 44.34 64.69 77.63	0.580 0.822 0.810 0.905	0.114 0.115 0.123 0.135	0.47 0.71 0.68 0.77	
420	115.34	1.194	0.119	1.07	

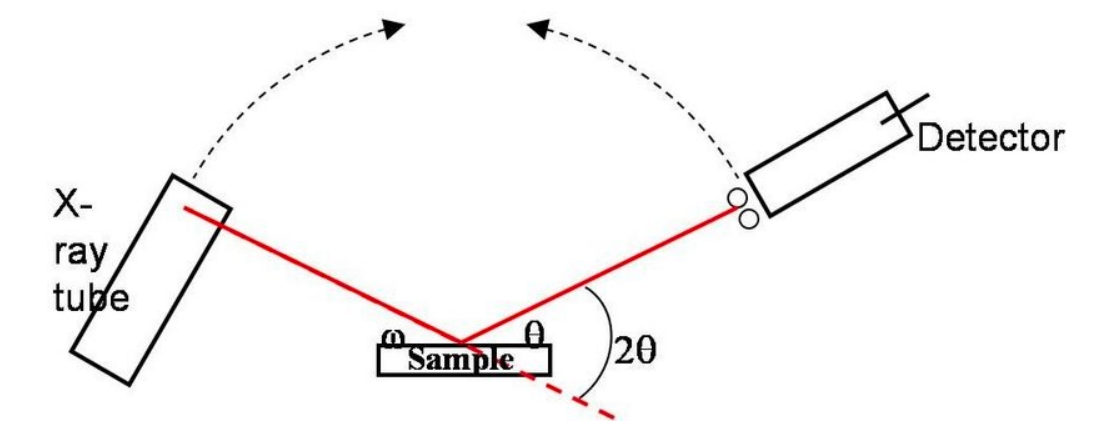
^a Materials Physics, Uppsala University, Ångströmlaboratoriet, Box 530, 75121 Uppsala, Sweden

^b Applied Crystallography Group, Department of Chemistry, University College London, 20 Gordon Street, London WC1H 0AI, UK

A few examples and case studies

Example: EPFL XRD instrument

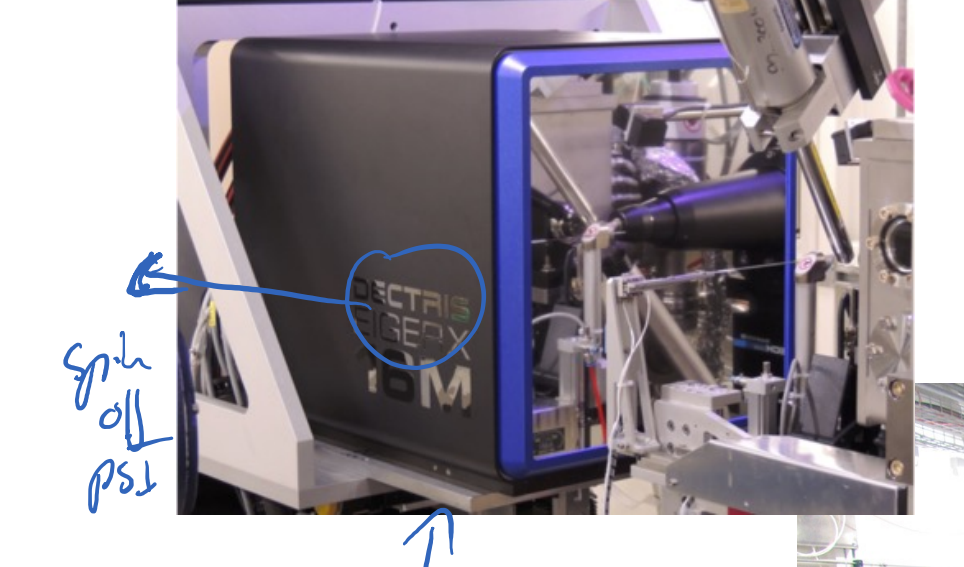




-> accessible as hold

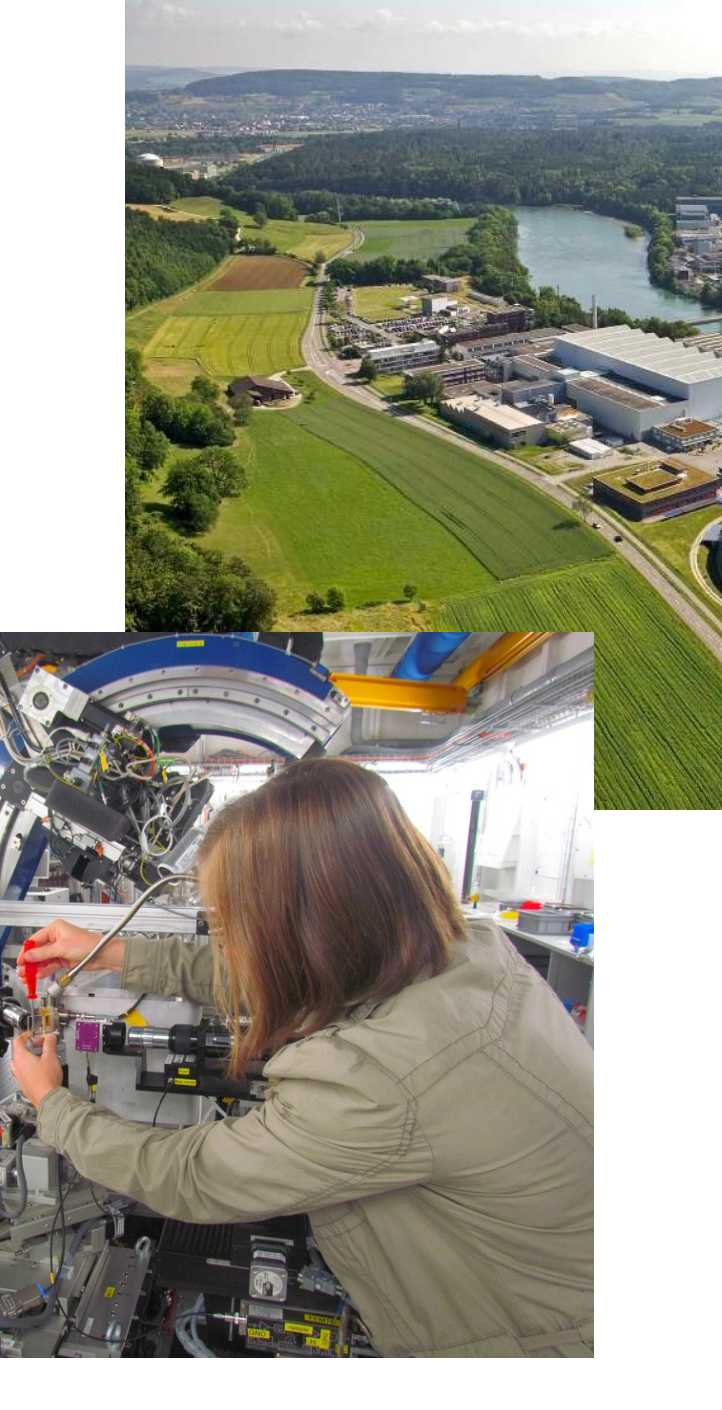
-> elective course as-txRD

Example Synchrotron Source



(expensu) ana delictis

de lient de servir de servir de la servir de



Some be-brus de lieotel to porche diff.

Villy

Example: In-operando battery research



den ; oh-gi-

Article

pubs.acs.org/JACS

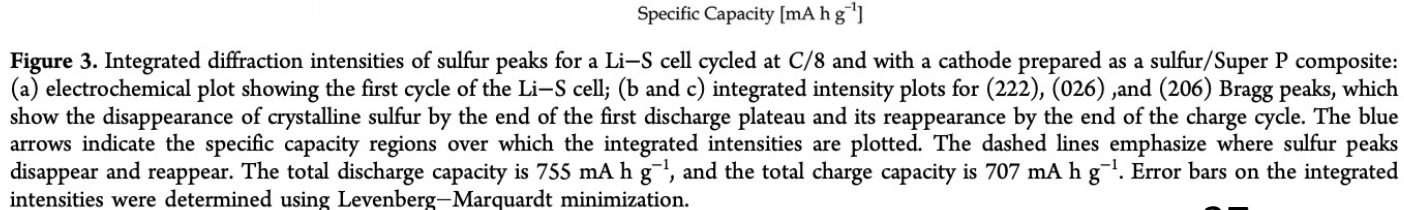
In Operando X-ray Diffraction and Transmission X-ray Microscopy of Lithium Sulfur Batteries

Johanna Nelson, †,‡,⊥ Sumohan Misra,†,⊥ Yuan Yang,§,⊥ Ariel Jackson,§ Yijin Liu,† Hailiang Wang,^{||} Hongjie Dai, || Joy C. Andrews,† Yi Cui,*,‡,§ and Michael F. Toney*,†,‡

-> new/alternative Su Hay cleans

-> studied / amphalgier chapes at on

-> Exp should regulation of S



1300

1350

1400

Crystalline sufur disappears 2.6 2.2 600 700 800 900 1000 1100 1200 1300 1400 Specific Capacity (mA h g⁻¹)

37

[†]Stanford Synchrotron Radiation Lightsource, and [‡]Stanford Institute for Materials and Energy Science, SLAC National Accelerator Laboratory, 2575 Sand Hill Road, Menlo Park, California 94025, United States

[§]Department of Materials Science and Engineering, and ^{||}Department of Chemistry, Stanford University, Stanford, California 94305, United States

Example: In operando – laser printing PSI

ARTICLE IN PRESS

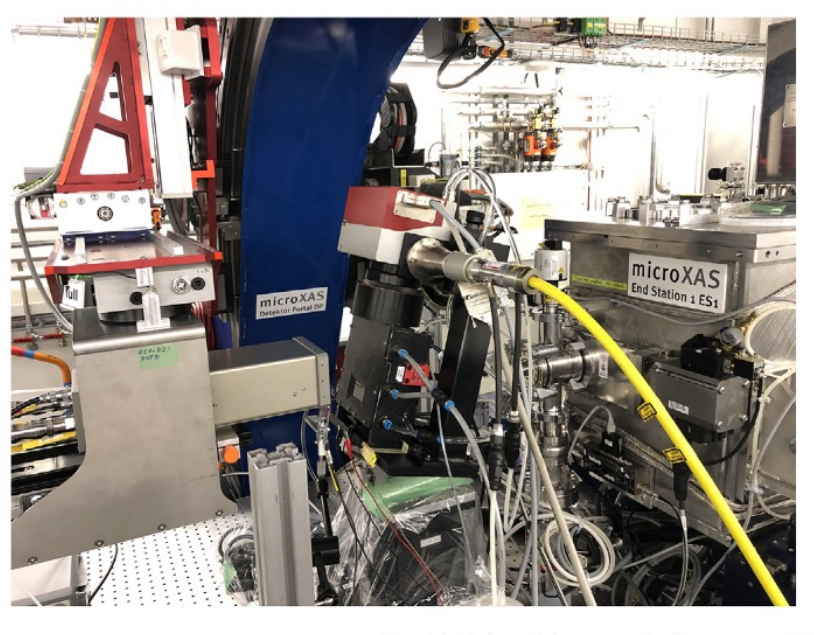
Materials Today • Volume xxx. Number xx • xxxx 2019

RESEARCH



Operando X-ray diffraction during laser 3D printing

Samy Hocine ^{1,2}, Helena Van Swygenhoven ^{1,2,*}, Steven Van Petegem ¹, Cynthia Sin Ting Chang ¹, Tuerdi Maimaitiyili ¹, Gemma Tinti ³, Dario Ferreira Sanchez ⁴, Daniel Grolimund ⁴, Nicola Casati ⁵



Materials Today ● Volume xxx, Number xx ● xxxx 2019

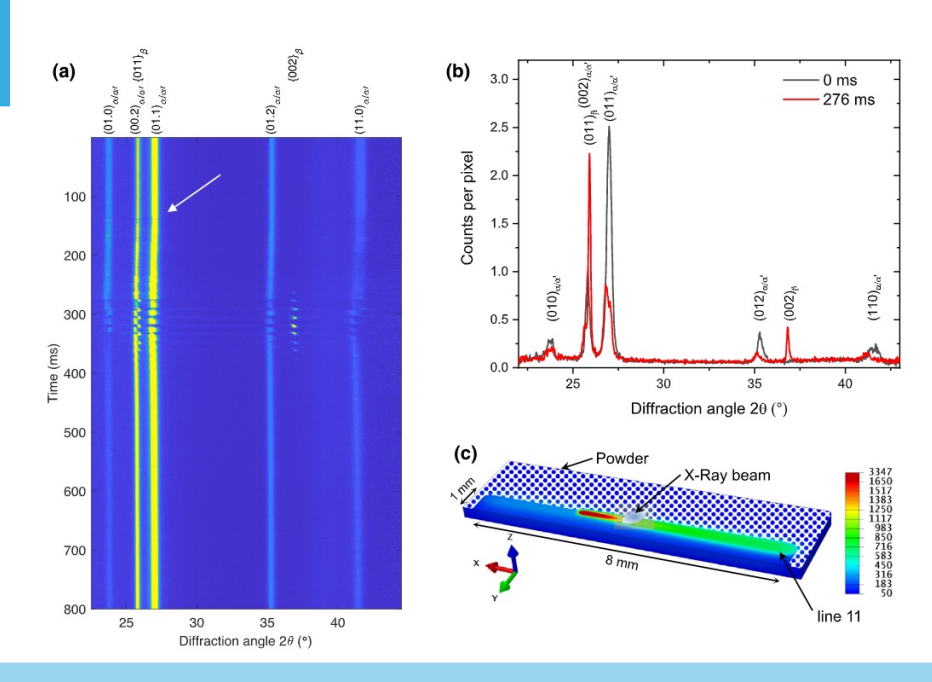


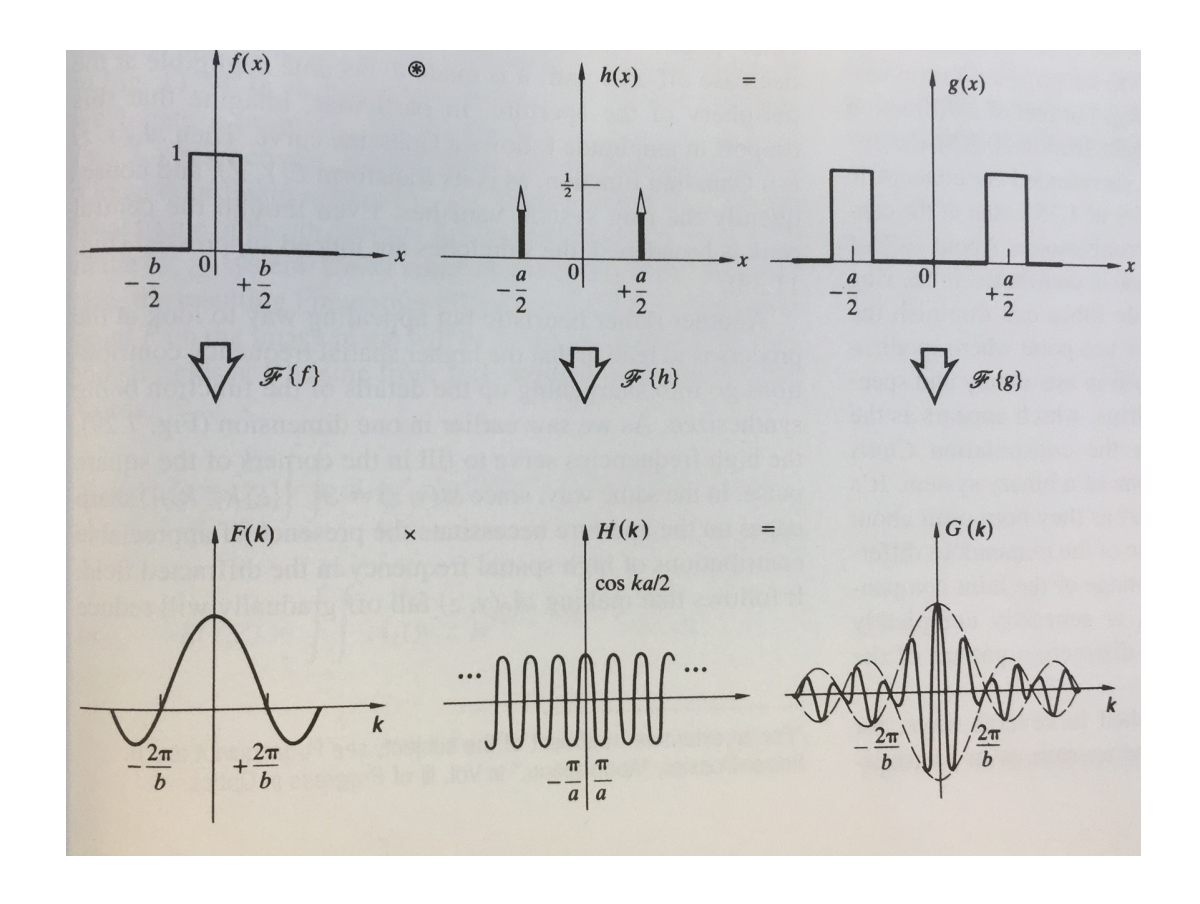
FIGURE 3

(a) Phase evolution during printing of a single layer, shown as an intensity vs. diffraction angle and time by stacking 16,000 individual diffraction patterns. The white arrow indicates the start of the printing process, (b) diffraction patterns recorded prior to printing and during printing of the 11th line at t = 276 ms, (c) schematic representation of the relative position of laser, X-ray beam and HAZ at t = 276 ms. (Temperature scale in degree Celsius).

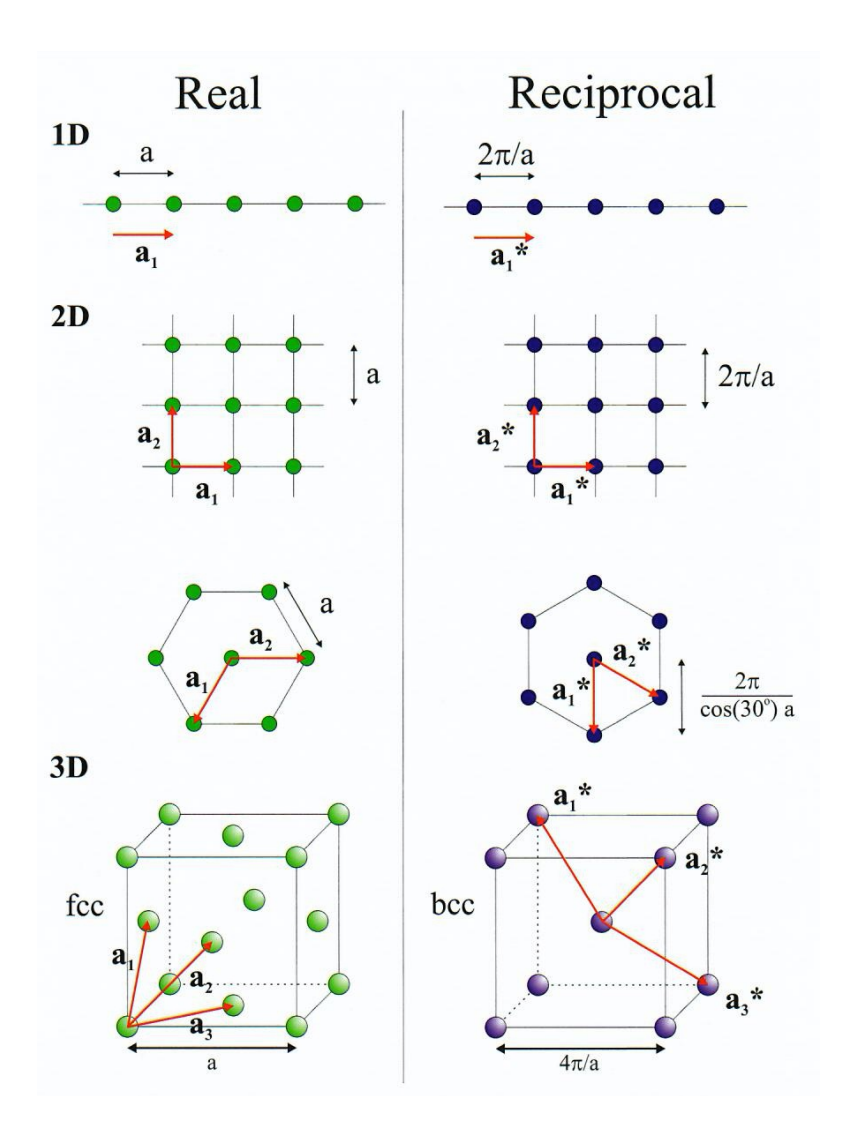
Outlook

Diffraction as Fourier Transform
Reciprocal Lattice
Bragg and Laue Diffraction
Structure Factor
Detailed Electronic Structure Maps

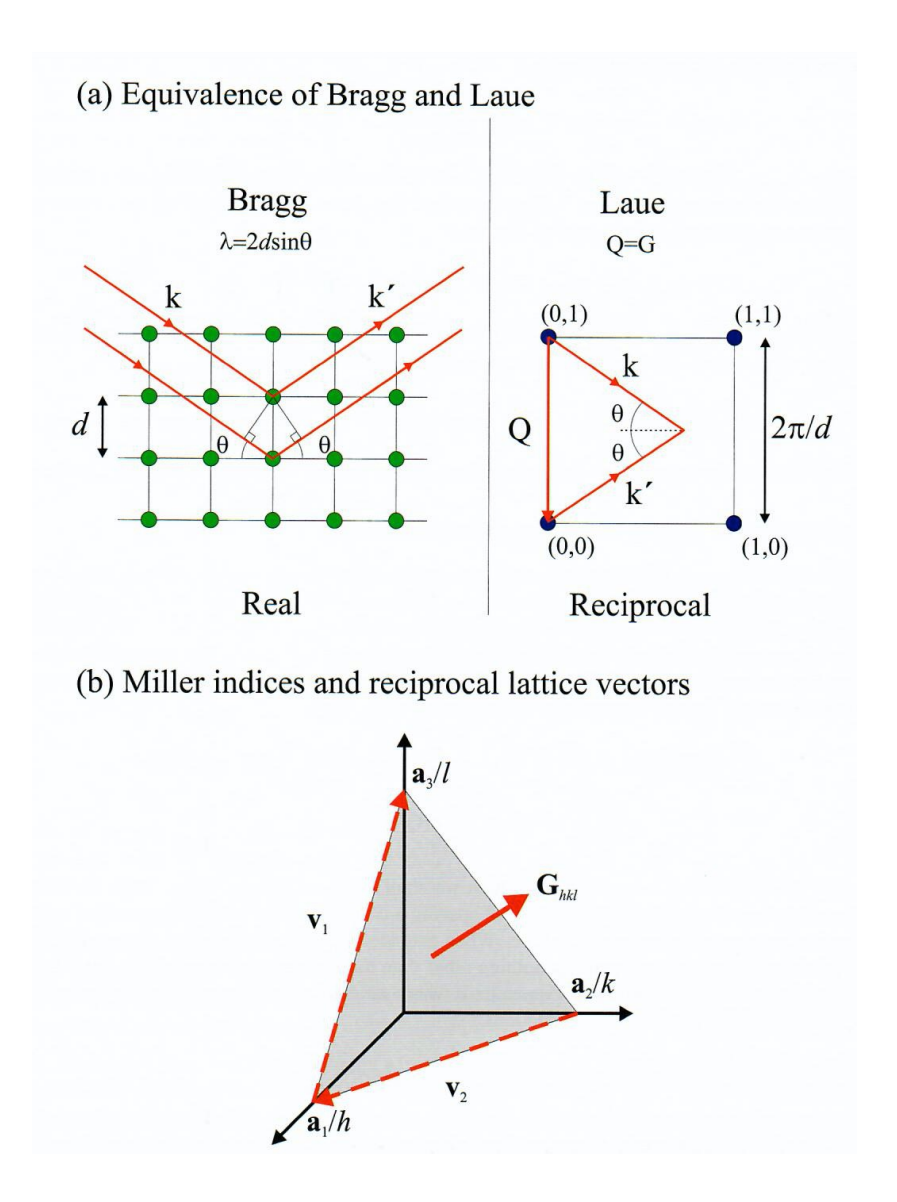
Diffraction as Fourier transform:



For each lattice a reciprocal lattice can be defined



Bargg and Laue conditions



The Nobel Prize in Physics 1914

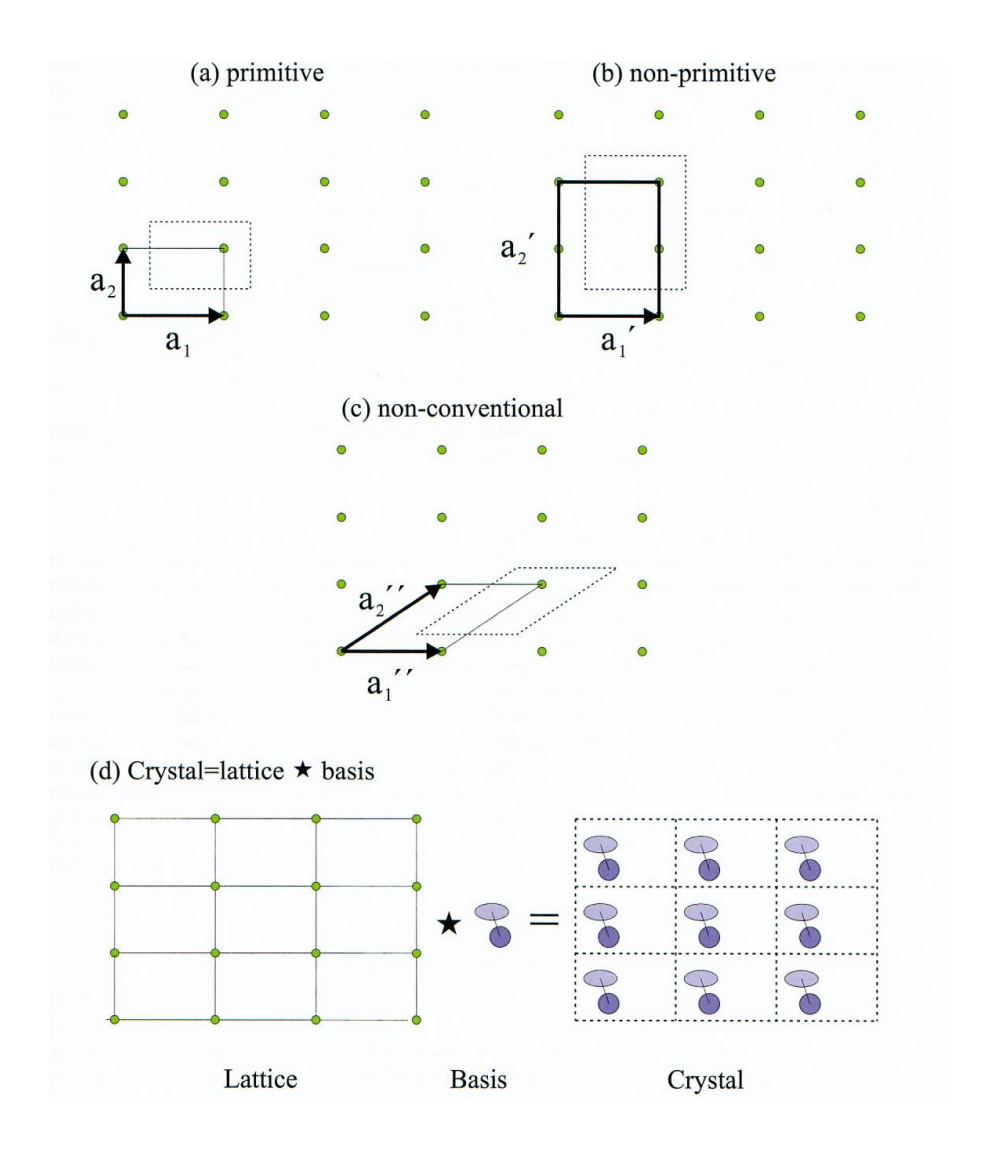


Photo from the Nobel Foundation archive.

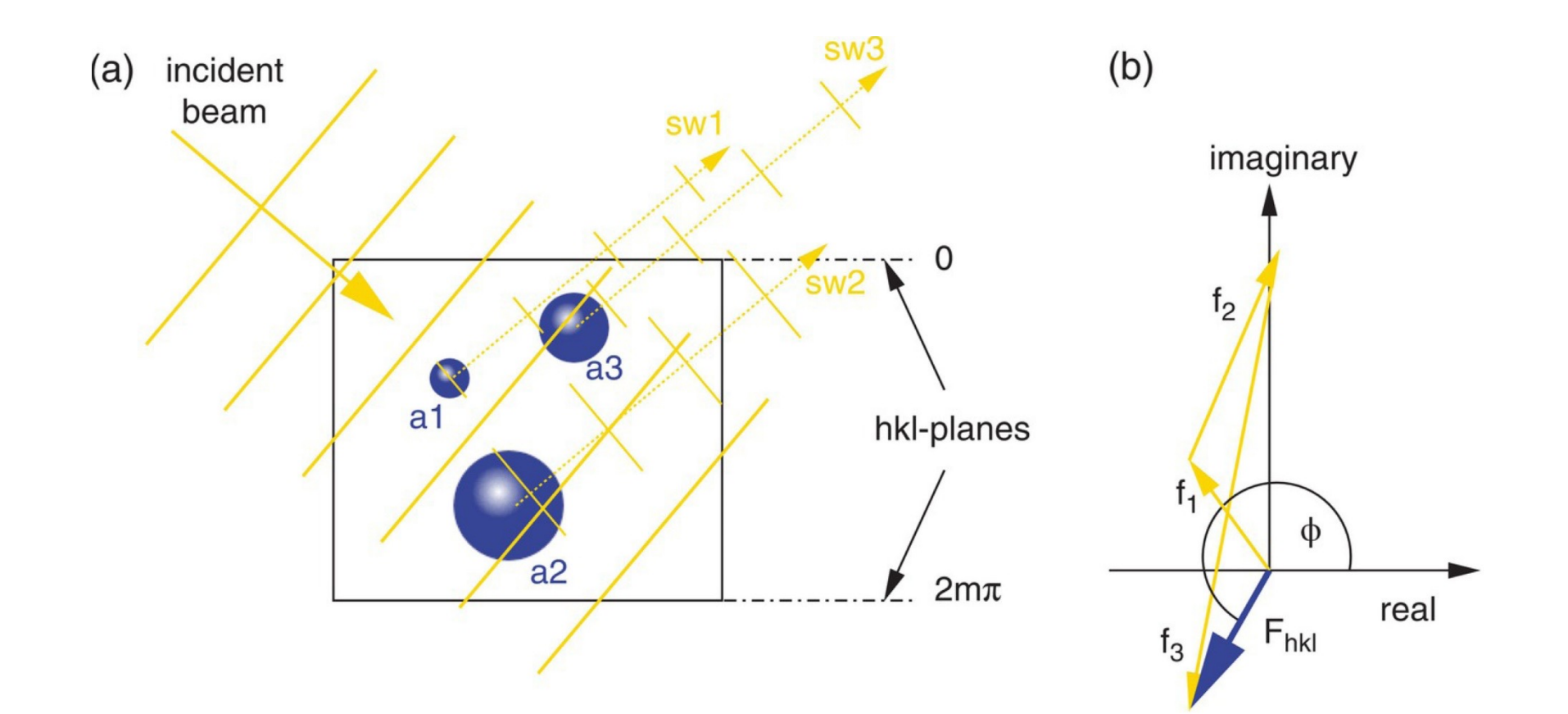
Max von Laue

Prize share: 1/1

A crystal is defined by ist lattice and basis



The structure factor



The end